nature chemical biology

ARTICLES

https://doi.org/10.1038/s41589-021-00787-6

Check for updates

Engineering AraC to make it responsive to light instead of arabinose

Edoardo Romano[1,2,3,6], Armin Baumschlager[4,6], Emir Bora Akmeriç[1,2], Navaneethan Palanisamy[1,2,3], Moustafa Houmani[4], Gregor Schmidt[4], Mehmet Ali Öztürk[1,2], Leonard Ernst[5], Mustafa Khammash[4]✉ and Barbara Di Ventura[1,2]✉

The L-arabinose-responsive AraC and its cognate P_{BAD} promoter underlie one of the most often used chemically inducible prokaryotic gene expression systems in microbiology and synthetic biology. Here, we change the sensing capability of AraC from L-arabinose to blue light, making its dimerization and the resulting P_{BAD} activation light-inducible. We engineer an entire family of blue light-inducible AraC dimers in *Escherichia coli* (BLADE) to control gene expression in space and time. We show that BLADE can be used with pre-existing L-arabinose-responsive plasmids and strains, enabling optogenetic experiments without the need to clone. Furthermore, we apply BLADE to control, with light, the catabolism of L-arabinose, thus externally steering bacterial growth with a simple transformation step. Our work establishes BLADE as a highly practical and effective optogenetic tool with plug-and-play functionality—features that we hope will accelerate the broader adoption of optogenetics and the realization of its vast potential in microbiology, synthetic biology and biotechnology.

Chemically inducible gene expression systems are invaluable tools with which to control biological processes for basic science as well as biotechnological applications. While allowing for tunability[1,2] and for a certain degree of spatial control[3], these systems have some limitations—they do not enable sophisticated spatio-temporal regulation and often lack reversibility or require washing steps to achieve it. These limitations can be overcome using light instead of small molecules as the external trigger. For example, with light, pulsatile inputs can be generated that alternate between dark (off) and maximum intensity (fully on), and have been shown to lead to effects that cannot be realized with light of graded intensity, such as reduced cell-to-cell variability in gene expression[4]. In fact, by adjusting the duty cycle (defined as the fraction of time that the light is fully on), the amount of cell-to-cell variability can be tuned, providing a new control modality for studying stochasticity in gene expression. This type of pulsatile input was also recently shown to enhance the biosynthesis of products in engineered cells, enabling a novel type of bioreactor operation in which enzyme expression is tuned to increase fermentation yield[5].

Several light-inducible gene expression systems are available for use in bacteria[6–12], some of which feature extremely high dark/light fold changes[10,11]. All these tools require the use of a specific promoter. In this Article, we aim to harvest the well-known and pervasive P_{BAD} promoter to allow optogenetic experiments to be performed with pre-existing plasmids and strains, without the need for cloning.

The P_{BAD} promoter regulates the *araBAD* operon, which encodes three enzymes that convert the sugar L-arabinose to D-xylulose-5-phosphate[13,14]. In the absence of L-arabinose, P_{BAD} is repressed by the transcriptional regulator AraC bound to the distal I_1 and O_2 half-sites, which causes the formation of a DNA loop that sterically blocks access of the RNA polymerase to the promoter (Fig. 1a). In the presence of L-arabinose, transcription from the P_{BAD} promoter is activated by AraC, which additionally negatively feeds back on its own promoter P_C[13,14]. Activation results from AraC binding to the adjacent I_1 and I_2 half-sites, which recruits the RNA polymerase (Fig. 1a). AraC is composed of an N-terminal dimerization domain (DD) and a C-terminal DNA binding domain (DBD) connected via a linker (Fig. 1b). Interestingly, AraC is always a homodimer, whether bound to arabinose or not[14]. Binding of arabinose triggers a conformational change in AraC, which results in the two DBDs being oriented in a way that favors their interaction with the I_1 and I_2 half-sites rather than the I_1 and O_2 half-sites (Fig. 1a)[13,14].

In this Article, we engineer an entire family of 'blue light-inducible AraC dimers in *Escherichia coli*' (BLADE). After characterizing BLADE in terms of kinetics, reversibility, spatial control and light dependence, we demonstrate that BLADE can be used to regulate, with light, previously constructed plasmids and strains, obtaining reversibility that cannot be achieved with L-arabinose. We show that BLADE functions by contacting the I_2 half-site within the P_{BAD} promoter in the lit state, while in the dark state aggregates are formed, which might contribute to the tightness of the system. Finally, we use BLADE to control the endogenous arabinose operon and direct *E. coli* growth on L-arabinose with blue light.

We envision that BLADE will stimulate the incorporation of optogenetic experiments in microbiology and will facilitate optogenetic endeavors in synthetic biology due to its compatibility with previously constructed strains and plasmids, its added functionality (which cannot be achieved easily with chemical inducers) and its reliable performance.

[1]Faculty of Biology, Institute of Biology II, University of Freiburg, Freiburg, Germany. [2]Centers for Biological Signalling Studies BIOSS and CIBSS, University of Freiburg, Freiburg, Germany. [3]Heidelberg Biosciences International Graduate School (HBIGS), University of Heidelberg, Heidelberg, Germany. [4]Department of Biosystems Science and Engineering, ETH Zürich, Basel, Switzerland. [5]BioQuant Center for Quantitative Biology, University of Heidelberg, Heidelberg, Germany. [6]These authors contributed equally: Edoardo Romano, Armin Baumschlager. ✉e-mail: mustafa.khammash@bsse.ethz.ch; barbara.diventura@bio.uni-freiburg.de

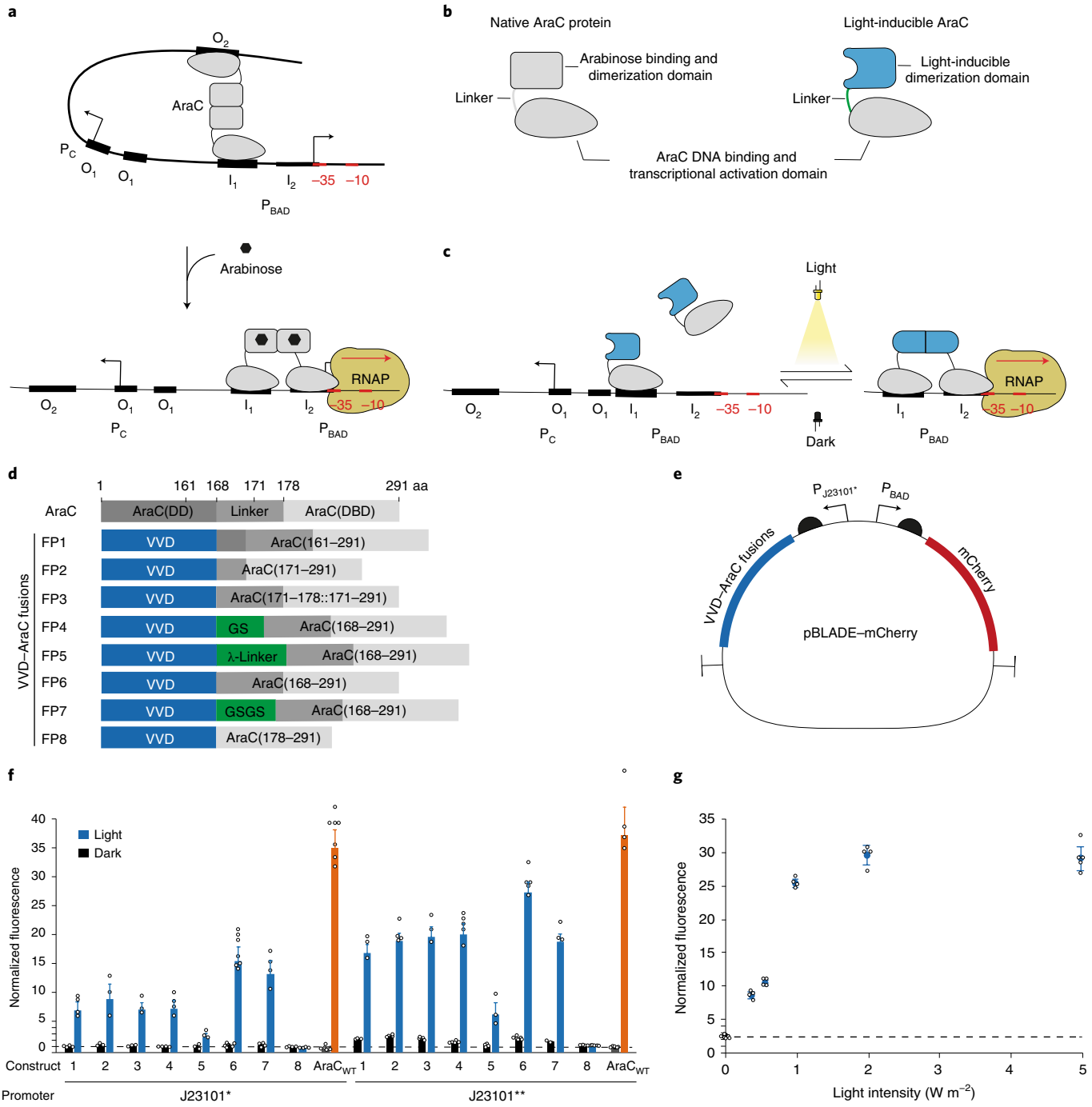

Fig. 1 | Engineering and characterization of a novel light-inducible AraC. a, Mechanism of arabinose-induced P_{BAD} induction by AraC. The thickness of the I_1 and I_2 half-sites symbolizes the affinity with which AraC binds to them. P_C, promoter driving the expression of *araC*. The −35 and −10 regions of the promoter are shown in red to differentiate them from the AraC binding sites. **b**, Domain composition of wild-type (left) and light-inducible (right) AraC. **c**, Expected mechanism of P_{BAD} activation by light-inducible AraC. **d**, Domain composition of the chimeric VVD–AraC DBD fusion proteins (FPs). In FP3, amino acids 171–178 of the natural linker are present twice. **e**, Plasmid for expression of a gene of interest (here mCherry) under control of BLADE. **f**, mCherry fluorescence intensity in *E. coli* MG1655 cells transformed with the library shown in **d**, grown for 4 h either in the dark or under 460-nm light (5 W m^{-2}) illumination. Native AraC cloned under the same constitutive promoters was used as a positive control ($AraC_{WT}$). The bars for AraC represent the values obtained without (gray) and with 0.1% (orange) arabinose for 4 h. J23101* and J23101** indicate two variants of the J23101 promoter with different strengths. **g**, mCherry fluorescence intensity measured in *E. coli* MG1655 cells transformed with the FP6 fusion driven by the J23101** promoter grown for 4 h under 460-nm light of the indicated light intensity (cyan) or kept in the dark for 4 h (black). In **f** and **g**, values are normalized to the mCherry fluorescence intensity measured in *E. coli* MG1655 cells transformed with pReporter_only (Supplementary Table 1; dashed line). The individual data points are the mean values of 10,000 single-cell flow cytometry events. In **f**, values represent mean ± s.d. of $n = 3$ (FP2*, FP3* FP5*, FP1**, FP7**, PC**), $n = 4$ (FP1*, FP4*, FP7*, FP8*, FP2**, FP3**, FP5**), $n = 5$ (FP4**, FP8**, PC**), $n = 6$ (FP6**), $n = 7$ (PC*) and $n = 9$ (FP6*) biological replicates acquired on more than three different days. *, construct driven by the J23101* promoter; **, construct driven by the J23101** promoter. In **g**, values represent mean ± s.d. of $n = 3$ (dark) and $n = 4$ (light) biological replicates acquired on three different days.

Results

Creation of chimeric VVD–AraC fusion constructs. Inspired by a previous study in which chimeric AraC constructs have been cloned to probe the role of the DD and DBD[15], we reasoned that, by exchanging the dimerization domain of AraC with a light-inducible dimerization domain (Fig. 1b), we would be able to control, with light, the switching of this engineered AraC from monomer to dimer (Fig. 1c). In its monomeric form, the engineered AraC would contact the high-affinity I_1 half-site[16], but not the low-affinity I_2 half-site, needed to recruit the RNA polymerase. Its function as a light-inducible transcription factor (TF) would depend on finding the appropriate linker supporting the correct orientation of the two DBDs after dimer formation, permissive of I_1–I_2 binding (Fig. 1c). For the light-triggered dimerization domain we at first selected Vivid (VVD), which has often been successfully used to control, with light, the dimerization of proteins of interest[17–20]. VVD senses blue light via the flavin adenine dinucleotide (FAD) chromophore[21]. Blue light triggers the formation of a cysteinyl-flavin adduct, which generates a new hydrogen-bond network that releases the N terminus (N-terminal cap) from the protein core and restructures it, creating a new dimerization interface[22,23]. We swapped the AraC dimerization domain with $VVD^{N56K/C71V}$, a double mutant shown to stabilize the dimer[18], and cloned seven constructs having different linkers between AraC(DBD) and VVD as well as one construct without linker (Fig. 1d). We removed the *araC* gene from pBAD33 and introduced two constitutive promoters of different strength (J23101* and J23101**) to drive the expression of the chimeric VVD–AraC(DBD) fusion constructs (Supplementary Fig. 1). For a reporter gene, we cloned *mCherry* downstream of the P_{BAD} promoter (Fig. 1e). As a positive control, we constructed the same plasmid carrying full-length AraC in place of the VVD–AraC fusion (Supplementary Fig. 2a and Supplementary Table 1), while the plasmid without any TF (pReporter_only) was constructed to serve as negative control to monitor leaky expression from P_{BAD} (Supplementary Fig. 2b and Supplementary Table 1). Flow cytometry analysis of *E. coli* MG1655 cells transformed with the small library of VVD–AraC fusions, as well as the negative and the positive controls, kept in the dark or illuminated with 460-nm light ($5\,W\,m^{-2}$) for 4 h, showed that all 14 VVD–AraC constructs having a linker between the two domains were light-inducible, despite being less optimal than full-length AraC (Fig. 1f). The fusion without linker (FP8) did not activate gene expression, regardless of its expression levels (Fig. 1f). Different linkers corresponded to different amounts of gene expression, with the longest linker being the least active. With the weaker constitutive promoter driving expression of the VVD–AraC(DBD) fusion constructs (J23101*), the levels of reporter expression in the dark approached those of the negative control, to which the values were normalized (Fig. 1f). The stronger constitutive promoter (J23101**) led to substantially higher expression of the reporter gene after blue light illumination for all constructs, albeit at the cost of increased leakiness in the dark (Fig. 1f). Nonetheless, for some of the fusions, the light/dark fold change was higher with this promoter. We named a generic member of this family BLADE and the pBAD33-derived corresponding expression plasmid pBLADE (Fig. 1e). Reporter gene expression can be tuned not only by selecting different promoters to drive the expression of BLADE (Fig. 1f), but also by applying different light intensities (Fig. 1g). Importantly, even the highest intensity used in our experiments ($5\,W\,m^{-2}$) is perfectly tolerated by the bacterial cells, so it can be safely used (Supplementary Fig. 3). To demonstrate that BLADE is useful to control the expression of functional *E. coli* proteins, and not just fluorescent reporters, we cloned several genes coding for proteins involved in cell division (MinD[24,25] and its mutant MinDΔ10[26]) and cell shape (MreB[27] and RodZ[28]) in place of mCherry into pBLADE. We transformed each construct into MG1655 *E. coli* cells and either exposed cells to 4 h of blue light illumination or kept them in the dark. In all cases, cells kept in the dark were indistinguishable from those transformed with pReporter_only, which served as a negative control (Extended Data Fig. 1, Supplementary Fig. 4 and Supplementary Video 1), demonstrating the tightness of BLADE. Light-induced overexpression of the selected proteins caused the expected phenotypes, while light itself had no effect (Extended Data Fig. 1).

Although the conventional L-arabinose-responsive AraC is better than BLADE in terms of fold change (Fig. 1f and Extended Data Fig. 2a,b), the latter benefits from the fact that light is not catabolized (Extended Data Fig. 2b) and that its utilization is not dependent on a series of cellular processes such as transport, thus leading to less heterogeneity within the population, especially at lower inductions (Extended Data Fig. 2c,d and Supplementary Fig. 5). Moreover, light can be easily removed, while arabinose is not easily washed out from cells (Extended Data Fig. 2e,f and Supplementary Fig. 6).

Spatial control of gene expression. One of the benefits of optogenetic induction is the ability to spatially modulate gene expression. To showcase how BLADE could be used to control the expression of a target gene only in selected cells, we cloned superfolder green fluorescent protein (sfGFP)[29] into pBLADE. *E. coli* MG1655 cells transformed with pBLADE–sfGFP were then applied to an agar pad and subjected to confocal microscopy to expose a limited area ($6.4\,\mu m^2$) to blue light every 5 min. After 3 h, sfGFP was expressed up to 6.7-fold more in the illuminated cells than in the surrounding non-illuminated cells (Supplementary Fig. 7). Another interesting application of light-inducible TFs that relies on the possibility to shine light on a plate in desired patterns is bacterial photography[30]. To assess the effectiveness of BLADE in this type of application, we covered one lawn of *E. coli* MG1655 cells transformed with pBLADE–sfGFP with a photomask depicting the 'Blade Runner' movie poster (Fig. 2a) and another one with the photomask reproducing Michelangelo's 'Creation of Adam' fresco (Supplementary Fig. 8). We illuminated the plates with blue light overnight, then took several microscopy pictures and stitched them together (Fig. 2b,d). The sensitive light response of BLADE yielded a good contrast, resulting in high-quality bacteriographs that allowed for the faithful reproduction of the details in the images, such as facial expressions (Fig. 2c).

BLADE is compatible with pre-existing plasmids and strains. The uniqueness of BLADE resides in the fact that it is based on the widely used P_{BAD} promoter. If BLADE outcompeted AraC for the activation of the P_{BAD} promoter in the absence of arabinose when AraC assumes the P_{BAD}-inhibiting conformation (Fig. 1a), previously constructed plasmids and strains could be employed to perform optogenetic experiments with a simple (co)transformation step to bring BLADE into the cells (Fig. 3a). We therefore cloned the BLADE-encoding gene into the well-known pTrc99a plasmid, into which we replaced the IPTG-inducible pTrc promoter with the constitutive J23101** one (giving rise to $pBLADE^{ONLY\_A}$; Supplementary Table 1). We then co-transformed $pBLADE^{ONLY\_A}$ and a previously constructed pBAD33–mCherry plasmid into MG1655 cells and compared the mCherry levels in this strain with those in MG1655 cells co-transformed with pBLADE–mCherry and an empty pTrc99a, allowing for use of the same two antibiotics. The mCherry reporter was activated with blue light in both strains, although the fold change was slightly lower when BLADE was used with a pre-existing pBAD33 due to the competition with apo-AraC (Fig. 3b).

Next, we took a previously constructed strain (KC717), where the endogenous promoter driving the expression of the *rodZ* gene has been exchanged with P_{BAD}[31]. In the absence of arabinose, the endogenous chromosomal copy of AraC inhibits transcription from P_{BAD}, so RodZ is not expressed and the cells are spherical[28,31–33].

Fig. 2 | BLADE allows for the production of high-contrast bacteriographs. a, Photomask used to produce the bacteriograph in **b** (printed with permission from Warner Bros. Entertainment). **b**,**d**, Bacteriographs. Two lawns of *E. coli* MG1655 cells transformed with pBLADE(FP6*) driving the expression of super folder GFP (sfGFP; pBLADE(FP6*)–sfGFP) were grown overnight at 37 °C while being exposed to blue light through the photomasks in **a** or Supplementary Fig. 8 (**b** and **d**, respectively). Bacteriographs were performed multiple times with similar results. In total, 110 (**b**) and 160 (**d**) individual images were taken with a fluorescent microscope and stitched together with Zen Blue 2.3 software. Scale bars in **b** and **d**, 1 cm. **c**, Zoom in on two parts of the bacteriograph shown in **b**. Scale bar, 300 µm.

In the presence of arabinose, endogenous AraC initiates transcription from P_{BAD} and, consequently, RodZ is expressed, leading to the reappearance of rod-shaped cells[31]. We transformed KC717 cells either with a modified pBLADE from which the P_{BAD} promoter and the *mCherry* gene were eliminated (pBLADE^{ONLY_C}, population A; Supplementary Table 1) or with an empty pBAD33 deprived of *araC* and P_{BAD}, which was used to allow growing of both strains in the presence of the same antibiotic (pCAM, population B; Supplementary Table 1) and either kept both populations uninduced (in the dark for population A and without arabinose for population B) or induced them for 4 h (with blue light for population A and with arabinose for population B). At this time point, population A recovered the rod shape to a greater extent than population B (Fig. 3c). To showcase the power of optogenetics to quickly switch induction off, we subjected the cells to a recovery phase by putting them into the dark (population A) and washing arabinose off (population B). Although it was possible to obtain spherical cells again after 2 h of dark incubation, the cells that had been induced with arabinose did not recover the initial phenotype and instead became even more rod-shaped (Fig. 3c).

BLADE aggregates in cells kept in the dark. Wild-type AraC and BLADE are substantially different in their mode of action. AraC is always a dimer that, in the absence of arabinose, binds the I_1 and O_2 half-sites and, in the presence of the sugar, binds the I_1 and I_2 half-sites (Fig. 1a). By contrast, BLADE is monomeric in the dark and dimeric under blue light illumination (Extended Data Fig. 3a,b). Although the conformation assumed by dimeric BLADE cannot be predicted easily, we know that it is able to contact the I_2 half-site, which is crucial for the recruitment of the RNA polymerase. Indeed, mCherry was not expressed in an illuminated sample in which the pBLADE plasmid was modified so that the I_2 half-site was in

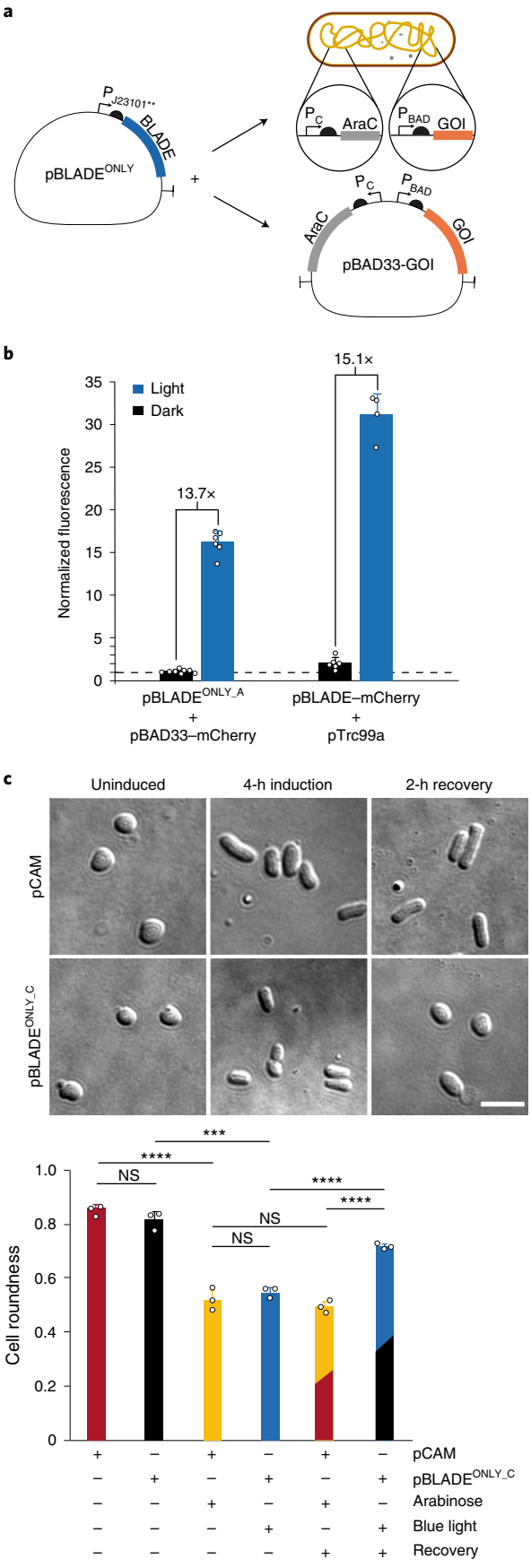

Fig. 3 | BLADE is compatible with pre-existing L-arabinose-responsive plasmids and strains. a, Schematic representation of the way in which BLADE can be used to control, with light, the expression of a gene of interest (GOI) previously put under L-arabinose control, either genomically or on a plasmid. **b**, mCherry fluorescence intensity in *E. coli* MG1655 cells co-transformed with the indicated plasmids grown for 4 h either in the dark or under 460-nm light (5 W m^{-2}) illumination. pBLADE^{ONLY_A}: pTrc99a deprived of the pTrc promoter expressing only BLADE. All values were normalized to the mCherry fluorescence intensity measured in *E. coli* MG1655 cells transformed with pReporter_only (Supplementary Table 1; dashed line). The individual data points are the mean values of 10,000 single-cell flow cytometry events. Values represent mean ± s.d. of $n = 8$ (pBLADE^{ONLY_A} + pBAD33-mCherry) and $n = 6$ (pBLADE-mCherry + pTRC99a) biological replicates acquired on three different days. **c**, Top: representative differential interference contrast (DIC) images of *E. coli* KC717 cells transformed with the indicated constructs at the indicated time points. Images were acquired on three independent days with similar results. pBLADE^{ONLY_C}: pBAD33 deprived of the P_{BAD} promoter expressing only BLADE. pCAM: empty pBAD33 deprived of the P_{BAD} promoter. Induction indicates 460-nm light (5 W m^{-2}) for the cells transformed with pBLADE^{ONLY_C} and 0.2% arabinose for the cells transformed with pCAM. Recovery indicates darkness for the cells transformed with pBLADE^{ONLY_C} and growth in a medium without arabinose for the cells transformed with pCAM. Scale bar, 5 µm. Bottom: quantification of cell roundness for the samples and conditions in the upper panel. Roundness is defined as $4 \times (\text{area})/(\pi \times (\text{major axis})^2)$. Values represent mean ± s.d. of $n = 3$ independent experiments. From left to right: $P = 0.05520$, $P = 0.00001$, $P = 0.00012$, $P = 0.18321$, $P = 0.19252$, $P = 0.00006$ and $P = 0.00004$. Not significant (NS) $P > 0.05$; ***$P < 0.001$; ****$P < 0.0001$. *P* values were calculated by the two-tailed, homoscedastic Student's *t*-test. In **b** and **c**, BLADE variant: FP6 driven by the J23101** promoter.

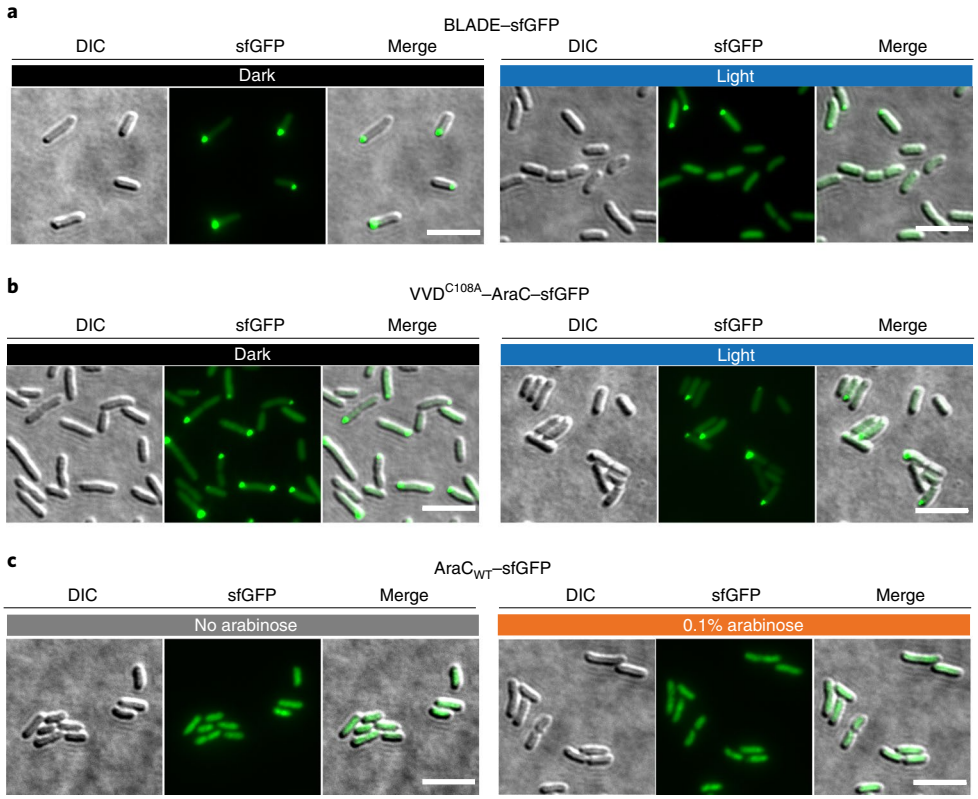

Fig. 4 | BLADE–sfGFP forms aggregates in the dark. a–c, Representative microscopy images of *E. coli* MG1655 cells expressing the indicated construct grown for 4 h in the dark (**a**,**b**, left panels) or in a medium without arabinose (**c**, left), or under 460-nm light (5 W m^{-2}) light (**a**,**b**, right) or in medium with 0.1% arabinose (**c**, right). Scale bar, 5 µm. Images were acquired on three days with similar results.

inverse orientation while the −35 region of the P_{BAD} promoter was left unchanged (Extended Data Fig. 3c,d).

To test whether BLADE is degraded in the dark in *E. coli* as shown for VVD in *Neurospora crassa*[34–36], we constructed a C-terminal sfGFP fusion to BLADE. We observed no difference between the steady-state GFP levels under the two conditions (Extended Data Fig. 4a). Assuming an equivalent constitutive rate of GFP production for cells, irrespective of the light input, these results suggest there is no differential degradation in the two conditions. Fluorescence microscopy, however, revealed the formation of aggregates in half of the cells kept in the dark (Fig. 4a and Extended Data Fig. 4b,c). The aggregates are due to the VVD moiety in BLADE, because a mutant BLADE with alanine in place of the adduct-forming cysteine (VVD^{C108A}) also showed aggregates under blue light illumination (Fig. 4b and Extended Data Fig. 4c), while wild-type AraC–sfGFP was cytoplasmic (Fig. 4c). Time-lapse fluorescence microscopy indicated that the aggregates do not disperse under blue light illumination, but are instead asymmetrically segregated during cell division (Supplementary Video 2). Newborn cells contain either no foci or foci much smaller than those found in cells kept in the dark (Supplementary Video 2).

Expanding the family of BLADE TFs. In principle, BLADE could have been designed using other light-inducible dimerization domains. Moreover, the position of this domain with respect to the DBD of AraC may not need to reflect that found in the wild-type protein. To test if other functional combinations with different characteristics could be identified, we generated a much larger set of samples for characterization. As a light-inducible dimerization unit, we included not only VVD, but also the light oxygen voltage (LOV) domain of *Vaucheria frigida* aureochrome1 (VfAu1)[37,38], which is naturally found C-terminally to a bZip DBD[38] and which, like VVD, homodimerizes upon blue light stimulation[39,40]. To assess the functionality of the chimeric transcription factors (cTFs), we used only the P_{BAD} promoter (I_1–I_2 half-sites) and removed the upstream regulatory elements (O_1 and O_2 half-sites[10]). We systematically explored how the expression levels of the cTF affected mCherry levels in the dark and after blue light illumination. We first used an IPTG-inducible promoter[41] to achieve various levels of expression of the cTFs, with the goal of finding the most appropriate expression level, which can subsequently be fixed using a constitutive promoter that matches the IPTG-induced transcription (Extended Data Fig. 5 and Supplementary Fig. 9). In principle, the optimal output might be achieved at intermediate cTF concentrations (Extended Data Fig. 5a). Here, we defined as output the light/dark fold change. However, depending on the application, other properties such as high output expression or low dark state might be more relevant. To meet our experimental needs, we developed a new device that is compatible with standard 96-well microtiter plates and that allows for fast high-throughput characterization (Extended Data Fig. 6a). In addition, we could test the N- and C-terminal positioning of the light-inducible dimerization unit, as well as different linkers connecting the two domains (Extended Data Fig. 6b). Using *E. coli* strain MG1655 *ΔaraCBAD ΔlacIZYA ΔaraE ΔaraFGH*, we tested the constructs in the library with variable order between AraC(DBD) and the light-inducible dimerization unit and explored a wide range of IPTG concentrations, from no induction to a concentration of 2 mM. For all constructs, the highest fold change was reached at intermediate mCherry expression levels (Fig. 5a). Placing AraC(DBD) at the C terminus led to higher fold changes for VVD-based constructs, mainly due to lower mCherry expression in the dark (Fig. 5b). For VfAu1, the opposite was true (Fig. 5c).

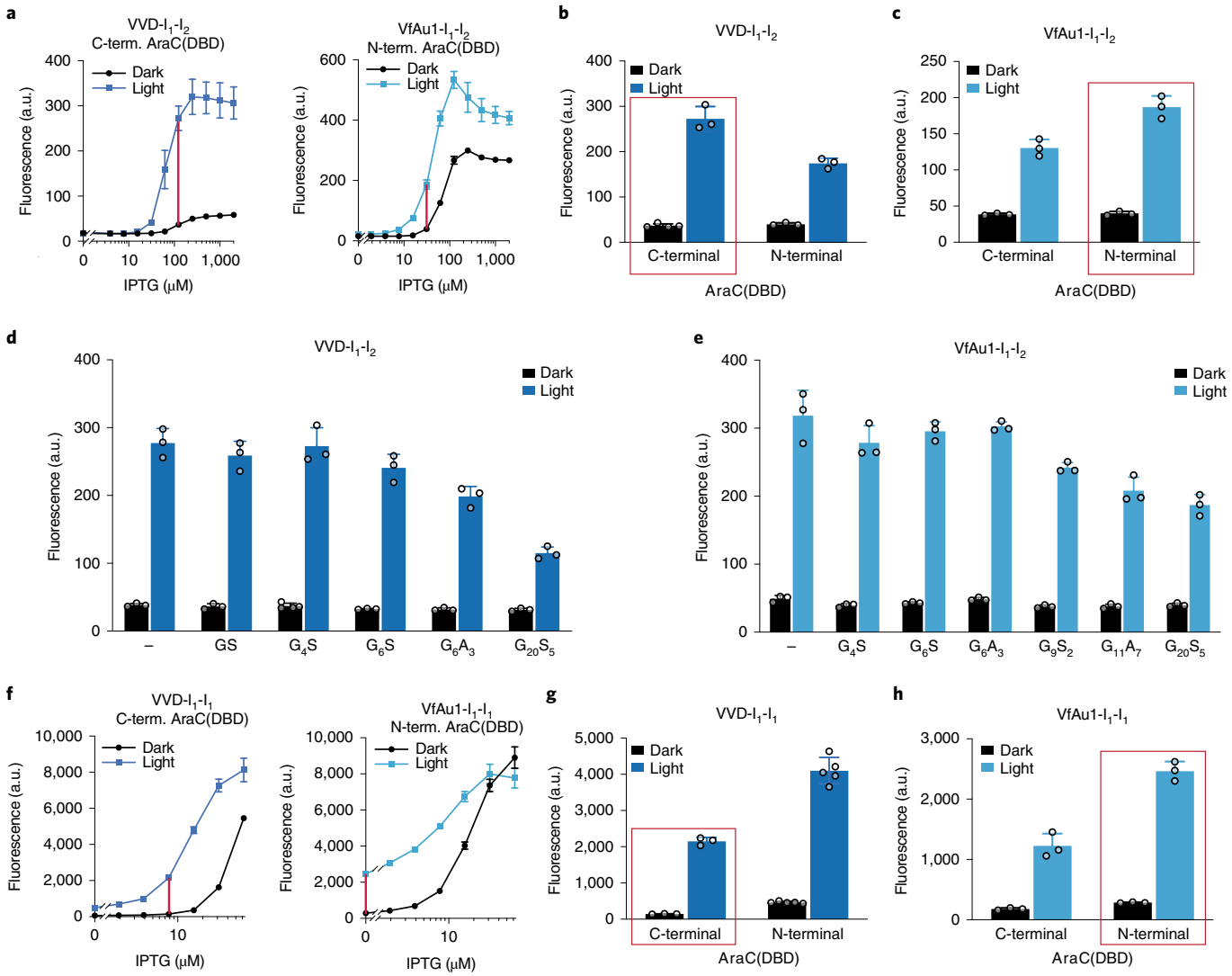

Fig. 5 | Engineering an optimized and expanded family of BLADE TFs. a, Examples of IPTG dose–response curves obtained with VVD::G_4S::AraC(DBD) and AraC(DBD)::$G_{20}S_5$::VfAu1. The highest light/dark fold change is indicated with a red line. **b**,**c**, Reporter gene fluorescence obtained with VVD::G_4S::AraC(DBD) (C-terminal) and AraC(DBD)::G_4S::VVD (N-terminal) (**b**) or VfAu1::$(G_4S)_5$::AraC(DBD) (N-terminal) and AraC(DBD)::$(G_4S)_5$::VfAu1 (C-terminal) (**c**) in the presence of 125 μM and 62.5 μM IPTG (**b**) or 125 and 31.25 μM IPTG (**c**), respectively. The red box indicates the samples for which the dose–response curve is shown in **a**. In Extended Data Figs. 7 and 8 we show the data obtained with AraC(DBD)::G_4S::VVD and VfAu1::$(G_4S)_5$::AraC(DBD), respectively. **d**,**e**, Reporter gene fluorescence obtained with a library of constructs with different linkers between C-terminal AraC(DBD) and VVD (**d**) or N-terminal AraC(DBD) and VfAu1 (**e**). The same IPTG concentration was used for all constructs (125 μM in **d** and 31.25 μM in **e**). For IPTG dose–response curves see Extended Data Figs. 7 and 8. **f**, Same as in **a**, but with a synthetic P_{BAD} promoter containing two copies of the I_1 half-site. The highest light/dark fold change is indicated with a red line. **g**, Same as in **b**, but with a synthetic P_{BAD} promoter containing two copies of the I_1 half-site; 7.8125 and 3.906 μM IPTG were used to induce the C- and N-terminal fusion constructs, respectively. See Supplementary Fig. 11 for the data obtained with AraC(DBD)::G_4S::VVD. **h**, Same as in **c**, but with a synthetic P_{BAD} promoter containing two I_1 half-sites; 15.625 μM and no IPTG were used to induce the expression of the C- and N-terminal fusion constructs, respectively. For the IPTG dose–response curve of VfAu1::$G_{20}S_5$::AraC(DBD) see Supplementary Fig. 12. In **g** and **h**, the samples in the red box are taken from the dose–response curve shown in **f**. All panels show the mCherry fluorescence intensity of MG1655 *ΔaraCBAD ΔlacIZYA ΔaraE ΔaraFGH* cells grown for 5 h either in the dark or under 465-nm light illumination (3.85 W m^{-2}). Values represent mean ± s.d. of $n = 3$, 4 and 5 biological replicates acquired separately in time.

Next, we investigated the effect of linker length on the cTFs. Based on the results obtained with the first library, we placed AraC(DBD) C-terminally for the VVD-based constructs, and N-terminally for those based on VfAu1. We selected a set of linkers from a previous report[42]. We also cloned variants without a synthetic linker for each of the dimerization domains. We found that synthetic linker lengths of up to seven and nine amino acids gave rise to the highest fold change for VVD and VfAu1, respectively (Fig. 5d,e). All these functional fusions expand the family of BLADE TFs. IPTG dose–response curves for all samples are provided in Extended Data Figs. 7 and 8.

We performed the same systematic characterization of BLADE family members using a synthetic P_{BAD} promoter, where the weak-affinity I_2 half-site was exchanged with a second copy of the high-affinity I_1 half-site (Supplementary Fig. 10), which is insensitive to arabinose as it is constitutively active when used with wild-type AraC[43]. The results with this promoter again showed the highest fold changes at no or low IPTG induction (Fig. 5f) and

were consistent with those obtained with the synthetic P_{BAD} promoter consisting only of the I_1 and I_2 half-sites, in which C- and N-terminal AraC(DBD) showed the highest fold change for fusions with VVD and VfAu1, respectively (Fig. 5g,h), although with higher maximal dark/light fold changes for the same cTFs compared to those obtained with the I_1–I_2 synthetic promoter. High IPTG concentrations led to toxic amounts of mCherry expression and were therefore indistinguishable for dark and light induction in most cases. IPTG dose–response curves for all samples are presented in Supplementary Figs. 11 and 12.

Controlling the L-arabinose metabolic pathway with light. AraC naturally controls the expression of genes that code for various proteins, such as transporters and other enzymes, necessary for the utilization of L-arabinose as carbon source[14,44,45] (Fig. 6a). Because these genes are under the P_{BAD} promoter, we reasoned that it would be possible to control L-arabinose catabolism with light in a strain depleted of AraC with a single transformation step to bring BLADE into the cells. We transformed two different BLADE versions bearing AraC(DBD) either N- or C-terminally (AraC(DBD)::G_4S::VVD and VVD::G_6S::AraC(DBD)) in *E. coli* MG1655*ΔaraC* (Fig. 6b, upper right). As a control, we used the *E. coli* MG1655*ΔaraCBAD* strain (Fig. 6b, upper left), which should not be able to catabolize L-arabinose due to lack of the AraA-B-D enzymes. We prepared cultures in M9 medium containing trace amounts of amino acids (0.0004% casamino acids) and either no or 2% L-arabinose, and incubated them at 37 °C either in the dark or under saturating blue light. Growth was measured at 40-min intervals using a spectrophotometer (Fig. 6c,d). Without the *araBAD* operon, no growth was detected in medium without arabinose after 18 h incubation in either the dark or blue light for strains containing either BLADE construct (Fig. 6b, lower left). In the presence of 2% L-arabinose, we observed a very small increase in absorbance for both dark and light-induced samples. This might be due to the low levels of promiscuity for L-arabinose utilization by other pathways. For the strain carrying the endogenous *araBAD* operon, there was no growth without L-arabinose, regardless of the presence of light (Fig.6b, lower right). By contrast, when 2% L-arabinose was present in the medium, growth was observed for both BLADE constructs for the illuminated samples (Fig. 6b, lower right). For BLADE with AraC(DBD) located at the N terminus, we observed a higher dark-state growth compared to that with the construct with C-terminal AraC(DBD), which confirms our previous characterization using the fluorescent protein. Comparison with *E. coli* MG1655*ΔaraCBAD* shows minimally increased growth for the dark expression (Supplementary Fig. 13), confirming the tightness of BLADE. Growth curves of individual samples are shown in Supplementary Figs. 14–17.

We also investigated how different expression levels of BLADE would impact growth on L-arabinose. Because of the altered growth conditions compared to the previous experiments, we again titrated the expression of BLADE with IPTG. As shown previously, the IPTG induction can ultimately be mapped to constitutive promoters for inducer-free light control (Extended Data Fig. 5). For both constructs, an intermediate IPTG concentration corresponded to the highest cell density (Fig. 6e and Extended Data Fig. 9a).

Finally, we grew *E. coli* MG1655*ΔaraC* cells transformed with the two BLADE constructs in a medium containing 2% L-arabinose with four IPTG concentrations, and either kept the cultures in the dark or exposed them to seven different light intensities (Fig. 6f and Extended Data Fig. 9b). The data show that, when using BLADE to control L-arabinose utilization, bacterial growth can be tuned by adjusting the light intensity, even if the amount of arabinose is fixed. Growth curves of individual samples are shown in Supplementary Figs. 18 and 19.

Discussion

AraC is among the best studied bacterial transcriptional regulators, and its cognate promoter P_{BAD} is one of the most widely used in microbiology, biotechnology and synthetic biology. We have developed BLADE, a family of AraC-derived TFs that activate transcription from the P_{BAD} promoter in response to blue light instead of arabinose. The uniqueness of BLADE as a light-inducible system lies in its compatibility with previously constructed L-arabinose-inducible plasmids and strains carrying the P_{BAD} promoter at an endogenous locus to drive the expression of a gene of interest. This makes it possible to readily perform optogenetic experiments without the need to construct anything new—a single transformation step is the only requirement (Fig. 3). We also demonstrated this by using BLADE to precisely activate the endogenous pathway for L-arabinose catabolism only with light (Fig. 6).

When the use of existing L-arabinose-inducible plasmids or strains is not paramount, light induction can be achieved by using pBLADE, a single plasmid bearing both BLADE and the P_{BAD} promoter followed by a multiple cloning site into which a gene of interest is cloned (Fig. 1e). The advantage of pBLADE compared to other previously constructed plasmids is that we created it using pBAD33 as a template (Supplementary Fig. 2a), so the resistance cassette and origin of replication of pBLADE are identical to those of pBAD33, which ensures compatibility with other previously constructed plasmids that should be co-transformed with pBLADE.

Recently, another pervasive chemically inducible gene expression system—one based on the *lac* operon—has been turned into a light-inducible one[46]. In this case, however, the LacI repressor itself was not engineered to sense light; rather, its expression was put under light control using the established pDawn optogenetic transcription system[6]. Consequently, this new system, called OptoLAC, requires a total of four proteins to achieve light inducibility. In contrast, light inducibility in BLADE is achieved more directly, and hence it does

Fig. 6 | Growth on L-arabinose can be controlled with light using BLADE TFs. a, Schematic representation of the operon involved in L-arabinose catabolism in *E. coli* and the principle behind BLADE-mediated control of the pathway. **b**, Top: schematic representation of the strains and plasmid used. Bottom: optical density at 600 nm of *E. coli* MG1655*ΔaraCBAD* cells transformed with AraC(DBD)::G_4S::VVD (N-terminal AraC(DBD)) and VVD::G_6S::AraC(DBD) (C-terminal AraC(DBD)) (left) and *E. coli* MG1655*ΔaraC* transformed with the same constructs (right) after incubation for 18 h at 37 °C either in the dark or under 465-nm light illumination (3.85 W m^{-2}). Cells were grown in M9 medium spiked with 0.0004% casamino acids without (−) or with 2% L-arabinose (+). All samples expressing the N-terminal fusion were induced with 62.5 μM IPTG, while those expressing the C-terminal fusion were induced with 125 μM IPTG. **c**,**d**, Growth curves of *E. coli* MG1655*ΔaraC* cells expressing AraC(DBD)::G_4S::VVD (N-terminal AraC(DBD)) (**c**) or VVD::G_6S:: AraC(DBD) (C-terminal AraC(DBD)) (**d**) in a medium containing 2% arabinose and 62.5 μM (**c**) or 125 μM (**d**) IPTG at 37 °C either in the dark or under 465-nm light (3.85 W m^{-2}). The red dashed lines indicate the time point at which growth values are shown in **b**. **e**, Optical density at 600 nm of *E. coli* MG1655*ΔaraC* cells expressing VVD::G_6S::AraC(DBD) grown in a medium containing 2% arabinose and the indicated IPTG concentrations for 18 h at 37 °C either in the dark or under 465-nm light (3.85 W m^{-2}). **f**, Optical density at 600 nm of *E. coli* MG1655*ΔaraC* cells expressing VVD::G_6S::AraC(DBD) grown in a medium containing 2% arabinose and the indicated IPTG concentrations for 17 h 20 min at 37 °C either in the dark or under 465-nm light of the indicated intensity. Values represent mean ± s.d. of $n = 3$ biological replicates acquired separately in time. Each data point shown in the bar plots represents a data point in a time course with measurements every 40 min, of which the average of the first three measurements was subtracted from all following time points to adjust for small differences in sample volume and inoculum. All time courses are shown in Supplementary Figs. 14–17 and 19.

not require additional circuitry. OptoLAC has inherent memory for a light input, a desirable features for certain applications. This same feature, however, is limiting when fast dynamics are needed. In this regard, BLADE offers more dynamic control over gene expression due to its immediate response to a light input through dimerization.

An important feature of BLADE is its minimal leakiness. Often, leakiness has been assessed by simply looking at the levels of reporter expression in the absence of the stimulus. However, this does not take into account whether the expression in the uninduced state is already too high compared to the expression in the absence of the regulator. In the case of BLADE, minimal leakiness was demonstrated by comparing its activity in the dark with expression obtained with the same plasmid deprived of the TF (pReporter_only; Fig. 1f and Extended Data Fig. 10). We put BLADE to the test by expressing several functional *E. coli* proteins whose overexpression causes morphological changes to the cells and showed that, in the dark, cells are indistinguishable from the control (Extended Data Fig. 1 and Supplementary Fig. 4). Minimal leakiness was also observed when controlling growth on L-arabinose with BLADE, as samples kept in the dark grew only slightly compared to the control cells lacking the pathway (Fig. 6b,e and Supplementary Fig. 13)

We also investigated the mechanism of BLADE-mediated gene expression and found that it involves dimer formation under blue light and subsequent contacting of the I_2 DNA half-site. Interestingly,

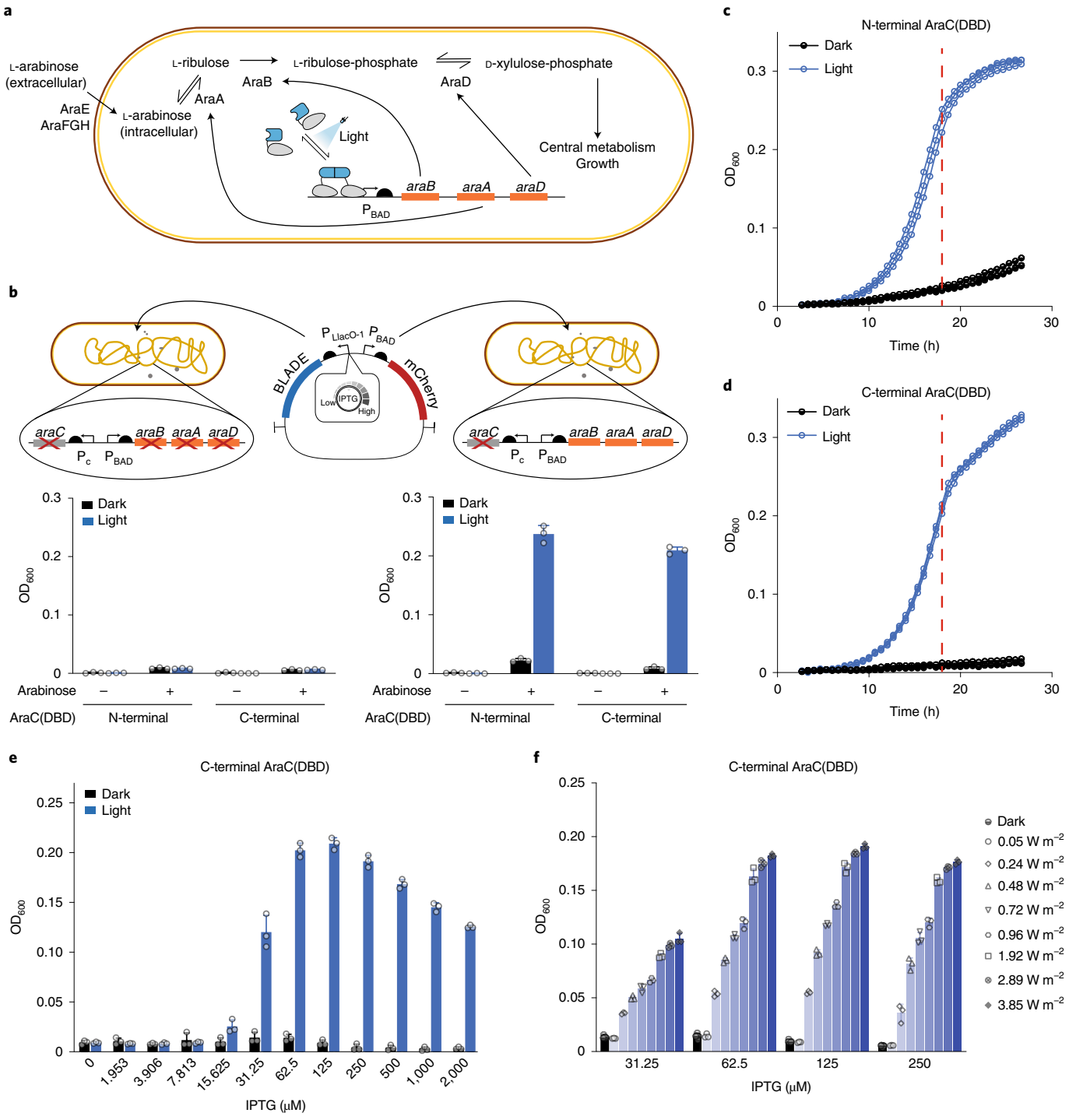

we discovered that BLADE localizes to aggregates in the dark in half of the cell population (Fig. 4a and Extended Data Fig. 4c), which we speculate might contribute to its tightness.

When engineering new TFs, we found that optimal functionality not only requires the careful engineering of the light-sensitive TFs themselves, but also proper calibration of their concentration. In particular, we found that, if the concentrations exceed certain levels, the functionality of the TF may in fact deteriorate (Fig. 5a) or disappear altogether (Fig. 5f). For the metric of light/dark fold change, intermediate TF expression levels always led to the highest values. Although we used IPTG to express a wide range of BLADE protein concentrations for this characterization, it is possible to have BLADE expressed constitutively at any of these concentrations for specific applications (Fig. 1f and Extended Data Fig. 5).

Beyond its favorable features, BLADE has some limitations, too. The maximum reporter gene expression level obtained with BLADE, while adequate for most applications, is not nearly as high as that reached with endogenous AraC or some other light-inducible systems[6,8,10,11]. Moreover, the off rate of any LOV domain-based tool is dictated by the time it takes for it to go back to the dark state and cannot be modulated with a second wavelength, as for phytochromes and phytochrome-related photosensors. Nevertheless, should faster off dynamics be needed for specific applications, mutations can be introduced to speed up the dark-state reversion of VVD[47].

Taken together, BLADE adds a valuable new tool with distinctive features to the growing arsenal of optogenetic gene expression systems. We envisage that BLADE's effectiveness as a transcriptional activator combined with its plug-and-play functionality, ease of use and low cost make it a compelling system that will contribute to the widespread adoption of optogenetic tools in the fields of microbiology, biotechnology and synthetic biology.

Online content

Any methods, additional references, Nature Research reporting summaries, source data, extended data, supplementary information, acknowledgements, peer review information; details of author contributions and competing interests; and statements of data and code availability are available at https://doi.org/10.1038/s41589-021-00787-6.

Received: 24 July 2020; Accepted: 19 March 2021;
Published online: 26 April 2021

References

1. Marschall, L., Sagmeister, P. & Herwig, C. Tunable recombinant protein expression in *E. coli*: promoter systems and genetic constraints. *Appl. Microbiol. Biotechnol.* **101**, 501–512 (2017).
2. Silva, J. P. N., Lopes, S. V., Grilo, D. J. & Hensel, Z. Plasmids for independently tunable, low-noise expression of two genes. *mSphere* **4**, e00340–19 (2019).
3. Kong, W., Blanchard, A. E., Liao, C. & Lu, T. Engineering robust and tunable spatial structures with synthetic gene circuits. *Nucleic Acids Res.* **45**, 1005–1014 (2017).
4. Benzinger, D. & Khammash, M. Pulsatile inputs achieve tunable attenuation of gene expression variability and graded multi-gene regulation. *Nat. Commun.* **9**, 3521 (2018).
5. Zhao, E. M. et al. Optogenetic regulation of engineered cellular metabolism for microbial chemical production. *Nature* **555**, 683–687 (2018).
6. Ohlendorf, R., Vidavski, R. R., Eldar, A., Moffat, K. & Moglich, A. From dusk till dawn: one-plasmid systems for light-regulated gene expression. *J. Mol. Biol.* **416**, 534–542 (2012).
7. Ramakrishnan, P. & Tabor, J. J. Repurposing synechocystis PCC6803 UirS-UirR as a UV-violet/green photoreversible transcriptional regulatory tool in *E. coli*. *ACS Synth. Biol.* **5**, 733–740 (2016).
8. Ong, N. T. & Tabor, J. J. A miniaturized *Escherichia coli* green light sensor with high dynamic range. *ChemBioChem* **19**, 1255–1258 (2018).
9. Jayaraman, P. et al. Blue light-mediated transcriptional activation and repression of gene expression in bacteria. *Nucleic Acids Res.* **44**, 6994–7005 (2016).
10. Baumschlager, A., Aoki, S. K. & Khammash, M. Dynamic blue light-inducible T7 RNA polymerases (Opto-T7RNAPs) for precise spatiotemporal gene expression control. *ACS Synth. Biol.* **6**, 2157–2167 (2017).
11. Li, X. et al. A single-component light sensor system allows highly tunable and direct activation of gene expression in bacterial cells. *Nucleic Acids Res.* **48**, e33 (2020).
12. Ding, Q. et al. Light-powered *Escherichia coli* cell division for chemical production. *Nat. Commun.* **11**, 2262 (2020).
13. Schleif, R. Regulation of the L-arabinose operon of *Escherichia coli*. *Trends Genet.* **16**, 559–565 (2000).
14. Schleif, R. AraC protein, regulation of the L-arabinose operon in *Escherichia coli*, and the light switch mechanism of AraC action. *FEMS Microbiol. Rev.* **34**, 779–796 (2010).
15. Bustos, S. A. & Schleif, R. F. Functional domains of the AraC protein. *Proc. Natl Acad. Sci. USA* **90**, 5638–5642 (1993).
16. Timmes, A., Rodgers, M. & Schleif, R. Biochemical and physiological properties of the DNA binding domain of AraC protein. *J. Mol. Biol.* **340**, 731–738 (2004).
17. Sheets, M. B., Wong, W. W. & Dunlop, M. J. Light-Inducible recombinases for bacterial optogenetics. *ACS Synth. Biol.* **9**, 227–235 (2020).
18. Wang, X., Chen, X. & Yang, Y. Spatiotemporal control of gene expression by a light-switchable transgene system. *Nat. Methods* **9**, 266–269 (2012).
19. Xu, X. et al. A single-component optogenetic system allows stringent switch of gene expression in yeast cells. *ACS Synth. Biol.* **7**, 2045–2053 (2018).
20. Chen, X. et al. An extraordinary stringent and sensitive light-switchable gene expression system for bacterial cells. *Cell Res.* **26**, 854–857 (2016).
21. Schwerdtfeger, C. & Linden, H. VIVID is a flavoprotein and serves as a fungal blue light photoreceptor for photoadaptation. *EMBO J.* **22**, 4846–4855 (2003).
22. Vaidya, A. T., Chen, C. H., Dunlap, J. C., Loros, J. J. & Crane, B. R. Structure of a light-activated LOV protein dimer that regulates transcription. *Sci. Signal.* **4**, ra50 (2011).
23. Zoltowski, B. D. & Crane, B. R. Light activation of the LOV protein vivid generates a rapidly exchanging dimer. *Biochemistry* **47**, 7012–7019 (2008).
24. de Boer, P. A., Crossley, R. E. & Rothfield, L. I. A division inhibitor and a topological specificity factor coded for by the minicell locus determine proper placement of the division septum in *E. coli*. *Cell* **56**, 641–649 (1989).
25. Di Ventura, B. et al. Chromosome segregation by the *Escherichia coli* Min system. *Mol. Syst. Biol.* **9**, 686 (2013).
26. Hu, Z. & Lutkenhaus, J. A conserved sequence at the C-terminus of MinD is required for binding to the membrane and targeting MinC to the septum. *Mol. Microbiol.* **47**, 345–355 (2003).
27. Wachi, M. & Matsuhashi, M. Negative control of cell division by *mreB*, a gene that functions in determining the rod shape of *Escherichia coli* cells. *J. Bacteriol.* **171**, 3123–3127 (1989).
28. Alyahya, S. A. et al. RodZ, a component of the bacterial core morphogenic apparatus. *Proc. Natl Acad. Sci. USA* **106**, 1239–1244 (2009).
29. Pedelacq, J. D., Cabantous, S., Tran, T., Terwilliger, T. C. & Waldo, G. S. Engineering and characterization of a superfolder green fluorescent protein. *Nat. Biotechnol.* **24**, 79–88 (2006).
30. Levskaya, A. et al. Synthetic biology: engineering *Escherichia coli* to see light. *Nature* **438**, 441–442 (2005).
31. Colavin, A., Shi, H. & Huang, K. C. RodZ modulates geometric localization of the bacterial actin MreB to regulate cell shape. *Nat. Commun.* **9**, 1280 (2018).
32. Bendezu, F. O., Hale, C. A., Bernhardt, T. G. & de Boer, P. A. RodZ (YfgA) is required for proper assembly of the MreB actin cytoskeleton and cell shape in *E. coli*. *EMBO J.* **28**, 193–204 (2009).
33. Shiomi, D., Sakai, M. & Niki, H. Determination of bacterial rod shape by a novel cytoskeletal membrane protein. *EMBO J.* **27**, 3081–3091 (2008).
34. Malzahn, E., Ciprianidis, S., Kaldi, K., Schafmeier, T. & Brunner, M. Photoadaptation in *Neurospora* by competitive interaction of activating and inhibitory LOV domains. *Cell* **142**, 762–772 (2010).
35. Heintzen, C., Loros, J. J. & Dunlap, J. C. The PAS protein VIVID defines a clock-associated feedback loop that represses light input, modulates gating, and regulates clock resetting. *Cell* **104**, 453–464 (2001).
36. Hunt, S. M., Elvin, M., Crosthwaite, S. K. & Heintzen, C. The PAS/LOV protein VIVID controls temperature compensation of circadian clock phase and development in *Neurospora crassa*. *Genes Dev.* **21**, 1964–1974 (2007).
37. Mitra, D., Yang, X. & Moffat, K. Crystal structures of aureochrome1 LOV suggest new design strategies for optogenetics. *Structure* **20**, 698–706 (2012).
38. Takahashi, F. et al. AUREOCHROME, a photoreceptor required for photomorphogenesis in stramenopiles. *Proc. Natl Acad. Sci. USA* **104**, 19625–19630 (2007).
39. Toyooka, T., Hisatomi, O., Takahashi, F., Kataoka, H. & Terazima, M. Photoreactions of aureochrome-1. *Biophys. J.* **100**, 2801–2809 (2011).
40. Grusch, M. et al. Spatio-temporally precise activation of engineered receptor tyrosine kinases by light. *EMBO J.* **33**, 1713–1726 (2014).

41. Lutz, R. & Bujard, H. Independent and tight regulation of transcriptional units in *Escherichia coli* via the LacR/O, the TetR/O and AraC/I_1–I_2 regulatory elements. *Nucleic Acids Res.* **25**, 1203–1210 (1997).
42. Chen, X., Zaro, J. L. & Shen, W. C. Fusion protein linkers: property, design and functionality. *Adv. Drug Deliv. Rev.* **65**, 1357–1369 (2013).
43. Reeder, T. & Schleif, R. AraC protein can activate transcription from only one position and when pointed in only one direction. *J. Mol. Biol.* **231**, 205–218 (1993).
44. Aidelberg, G. et al. Hierarchy of non-glucose sugars in *Escherichia coli*. *BMC Syst. Biol.* **8**, 133 (2014).
45. Lee, N. L., Gielow, W. O. & Wallace, R. G. Mechanism of araC autoregulation and the domains of two overlapping promoters, Pc and PBAD, in the L-arabinose regulatory region of *Escherichia coli*. *Proc. Natl Acad. Sci. USA* **78**, 752–756 (1981).
46. Lalwani, M. A. et al. Optogenetic control of the *lac* operon for bacterial chemical and protein production. *Nat. Chem. Biol.* **17**, 71–79 (2021).
47. Zoltowski, B. D., Vaccaro, B. & Crane, B. R. Mechanism-based tuning of a LOV domain photoreceptor. *Nat. Chem. Biol.* **5**, 827–834 (2009).

Methods

Strains, media and reagents. The strains used in this study are listed in Supplementary Table 2. For the experiments shown in Figs. 1, 3b and 4, Extended Data Figs. 1d–f, 2 and 4 and Supplementary Figs. 3, 5 and 6, the cultures were grown in autoclaved tryptone broth (TB; 10 g l^{-1} tryptone, 5 g l^{-1} NaCl, 1 mM NaOH). For the experiments shown in Figs. 2 and 3c and Extended Data Fig. 1b,c, the cultures were grown in autoclaved LB–Miller medium. For the experiments shown in Figs. 5 and 6, Extended Data Figs. 5, 7 and 8, and Supplementary Figs. 11 and 12, the cultures were grown in autoclaved LB–Miller medium for strain propagation and in sterile-filtered M9 medium supplemented with 0.2% casamino acids, 0.4% glucose, 0.001% thiamine, 0.00006% ferric citrate, 0.1 mM calcium chloride and 1 mM magnesium sulfate for all gene expression experiments. For the experiments shown in Supplementary Fig. 7 and Supplementary Video 2, the cultures were grown in tethering buffer (10 mM potassium phosphate, 0.1 mM EDTA, 1 mM L-methionine and 10 mM sodium lactate; pH 7.0). In experiments in which plasmids had to be maintained, the medium was supplemented with either 34 µg ml^{-1} chloramphenicol or 100 µg ml^{-1} ampicillin and 34 µg ml^{-1} chloramphenicol (Sigma-Aldrich Chemie). IPTG, rifampicin and doxycycline were purchased from Sigma-Aldrich Chemie.

Constructions of strains and plasmids. To integrate *lacY* expressed from the *rrnB P1* promoter into the *attB* site of *E. coli* BW25113[48,49] and to delete *araC* and *araBAD*, we used *λ* integrase expressed from pJW27[50]. The corresponding DNA containing a flippase recognition target (FRT)-flanked *kanR* from pKD13 for selection was transformed as linear DNA into *E. coli* BW25113 or MG1655 K-12 (ATCC 47076)[51] and selected at 30 °C on LB–agar plates containing chloramphenicol for expression of *λ* integrase. A single colony was used to inoculate 5 ml of LB medium containing chloramphenicol, and the culture was grown at 30 °C in a water bath with shaking. The cells were then moved to 42 °C for 15 min, before incubation on ice for 15 min.

Cloning was performed with NEBuilder HiFi DNA Assembly (New England Biolabs) or restriction enzymes. Detailed information about all the primers, backbones and inserts used in the cloning is provided in Supplementary Dataset 1. All polymerase chain reactions (PCRs) were performed using Phusion Flash High Fidelity PCR Master Mix (Thermo Scientific). Oligonucleotides were obtained from Sigma-Aldrich. Ligation reactions were transformed into chemically competent *E. coli* TOP10 cells.

To clone the extended library of BLADE TFs, we used a modular Golden Gate cloning strategy using an optimized junction set for part assembly taken from ref. [52]. The overhangs as well as the individual parts and the final plasmid sequences are shown in Supplementary Datasets 2 and 3. To invert the transcriptional unit containing the *mCherry* gene under AraC-controlled promoters, we first assembled the transcriptional unit separately, and then PCR-amplified the resulting fragment to create an A junction inverted at the end and an F junction inverted at the beginning of the transcriptional unit, and further treated the resulting construct as a part. Individual parts were first cloned into a part vector using BbsI-HF. The final plasmids were assembled from individual parts with BsaI-HF for digestion of the parts and BbsI-HF for digestion of the plasmid backbone, which contains a p15a and a chloramphenicol acetyl transferase. Plasmids were transformed using a one-step preparation protocol of competent *E. coli* cells for transformation of plasmids in testing strains[53]. The sequences of all cloned plasmids were confirmed by Sanger sequencing (Eurofins Genomics Europe Sequencing and Microsynth AG). A list of all vectors used and constructed in this study is provided in Supplementary Table 1 and Supplementary Dataset 3. Oligonucleotide sequences used for PCR amplification and Golden Gate part sequences are shown in Supplementary Datasets 2 and 4. The cloning was performed using chemically competent *E. coli* TOP10 cells (Thermo Scientific).

Bacterial growth. For the experiments shown in Figs. 1–4, Extended Data Figs. 1–4 and Supplementary Figs. 3–7, cultures were handled under safe red light whenever containing light-sensitive constructs. The cultures were incubated overnight in TB or LB medium and grown at 37 °C in an incubator shaking at 250 r.p.m., in a black plastic tube (Argos Technologies LiteSafe, 15 ml) if containing light-sensitive samples or in transparent glass tubes otherwise. The following morning, the cultures were diluted to an optical density at 600 nm (OD_{600}) of 0.1 and allowed to grow until $OD_{600} = 0.4$. Half of the culture was then transferred in transparent glass tubes and induced either with blue light or with arabinose for 4 h. For the experiments shown in Figs. 5 and 6, Extended Data Figs. 5, 7 and 8 and Supplementary Figs. 11–19, cultures were grown in an environmental shaker. The shaking incubator consisted of a Kuhner ES-X shaking module (Adolf Kühner AG) mounted inside an aluminum housing (Tecan) and temperature-controlled using an 'Icecube' (Life Imaging Services). Cultures were grown at 37 °C with shaking at 300 r.p.m. in black, clear-bottomed 96-well plates (Cell Culture Microplates 96 Well µClear CELLSTAR, Greiner Bio-One, cat. no. 655090), which were sealed with pierceable foil (Sealing foil, clear pierceable thin seal for PlateLoc, cat. no. 17318-001, Agilent) for fluorescent reporter expression and peelable foil (Sealing foil, clear peelable for PlateLoc, cat. no. 16985-001, Agilent) for growth experiments to prevent liquid evaporation and guarantee sterility, as well as a plastic lid (Greiner Bio-One, cat. no. 656171). Overnight cultures were inoculated in M9 medium and grown overnight to an OD_{600} of ~4. These cultures were diluted 1:20,000 into fresh M9 medium containing the respective inducer concentrations, immediately before the start of the experiment. This high dilution ensures that the cells are still in logarithmic growth phase after 5 h, at the end of the experiment[54]. Volumes of 200 µl of inoculated culture were incubated per well in the 96-well plates. Cells were grown for 5 h before transcription and translation were stopped with rifampicin and tetracycline[10]. The inhibition solution contained 500 µg ml^{-1} rifampicin and 50 µg ml^{-1} tetracycline in PBS (Sigma-Aldrich Chemie, Dulbecco's PBS) and was filtered using a 0.2-µm syringe filter (Sartorius). The 100-µl inhibition solution was aliquoted in 96-well U-bottom plates (Thermo Scientific Nunc), precooled on ice and samples were added in equal volumes (100 µl), resulting in a final inhibitor concentration of 250 µg ml^{-1} rifampicin (Sigma-Aldrich Chemie) and 25 µg ml^{-1} tetracycline (Sigma-Aldrich Chemie). After the sample was added, the solution was incubated on ice for at least 30 min. Then mCherry maturation was carried out at 37 °C for 90 min. The samples were kept at 4 °C until measurement with flow cytometry.

Light illumination systems. To illuminate the glass tubes in the shaker, six high-power 460-nm LEDs (type CREE XP-E D5-15, LED-TECH.DE) were used (Supplementary Fig. 20). The LEDs were connected to a power supply (Manson HCS-3102) that allowed the voltage to be tuned, and hence the light intensity. Unless specified, the light intensity reaching the cultures was 5 W m^{-2}, as measured with a LI-COR LI-250A light meter. For the bacterial photography, we used a custom-made light box with, among others, six blue (455 nm) LEDs (Supplementary Fig. 21). To avoid the generation of a blurred image in the bacteriograph, all the LEDs except the one in the center were obscured with colored tape. The average light intensity reaching the plate was 1.3 W m^{-2}.

Although another light plate was available[54], we designed a new 96-well plate to meet our experimental requirements. The 96-LED array was designed using CircuitMaker 1.3.0 (www.circuitmaker.com). The LEDs (SK6812, Dongguang Opsco Optoelectronics) were arranged on the printed circuit board (PCB) at a pitch of 9 mm in an 8 × 12 grid to be compatible with standard 96-well plates. All LEDs were daisy-chained using their D_{IN} and D_{OUT} ports. A 0.1-nF capacitor was placed in parallel with the V_{DD} port of each LED as proposed by the manufacturer. The two-layer circuit was manufactured on a 1.6-mm-thick FR-4 substrate, and the surface of the PCBs was coated with black solder mask to reduce reflection. The PCBs were ordered preassembled with the LEDs and 0.1-nF capacitors (www.pcbway.com). Every 96-LED PCB had one signal-in and one signal-out SubMiniature version A (SMA) connector such that several 96-LED PCBs could be daisy-chained using SMA cables and controlled by a single microcontroller. Up to 4 × 96-LED PCBs could be powered using a single Adafruit #658 5-V 10-A switching power supply (digikey.ch) using a custom-made PCB to distribute the power to several LED arrays. The LEDs were controlled by an Arduino Uno microcontroller (Arduino) using the fastLED library (http://fastled.io/).

The 96-LED array was mounted inside the shaking incubator using custom three-dimensional (3D)-printed holders. The holders were printed with an Ultimaker S5 using black Ultimaker co-polyester (Ultimaker) to reduce reflections. For better dissipation and distribution of the heat generated by the LEDs, a custom-made anodized aluminum plate (10-mm thick, with 96 holes of 4-mm diameter) was mounted on top of the 96-LED array. Another 3D-printed adapter was placed between the aluminum plate and the microtiter plate to ensure optical insulation of the wells. The 3D-printed parts and the metal plate were aligned and held in place by metal rods (4-mm diameter, 20-mm length).

Flow cytometry. For the experiments shown in Figs. 1 and 3, Extended Data Figs. 1–4 and Supplementary Figs. 3, 5 and 6, fluorescence was measured using an LSR Fortessa flow cytometer (BD Biosciences). Samples were centrifuged at 4,000*g* for 4 min to remove the glycerol-containing solution, then the pellets were resuspended in PBS. Data analysis was performed using the open-source FCSalyzer software (v. 0.9.1.5 α). This software was also used to calculate the mean fluorescence and the coefficient of variation (CV) for each sample. The mCherry fluorescence was excited with a 561-nm laser (50 mW), and emission was detected using a 610/20-nm filter pass (photomultiplier tube (PMT) voltage set to 750 V). The GFP fluorescence was excited with a 488-nm laser (100 mW), and emission was detected using a 530/30-nm filter pass (PMT voltage set to 405 V). A forward scatter height (FSC-H) threshold of 1,400 was used to gate for living cells and eliminate debris. A total of 10^5 events per sample were recorded for each experiment. The cell density of the samples was manually regulated by addition of PBS so as to have fewer than 2×10^4 events per second recorded by the machine. To compensate any variable that could alter measurement of the fluorescence by the flow cytometer, each experiment was normalized with the fluorescence value of the negative control grown the same day of the experiment. For the experiments shown in Fig. 5, Extended Data Figs. 5, 7 and 8 and Supplementary Figs. 11 and 12, fluorescence was measured on a Cytoflex S flow cytometer (Beckman Coulter) equipped with CytExpert 2.1.092 software. The mCherry fluorescence was excited with a 561-nm laser and emission was detected using a 610/20-nm bandpass filter and the following gain settings: forward scatter 100, side scatter 100, mCherry gain 700 when mCherry was expressed from the I_1–I_2 promoter, and 100 gain when mCherry was expressed from the I_1–I_1 promoter due to the difference in expression

levels. Thresholds of 2,500 FSC-H and 1,000 side scatter height (SSC-H) were used for all samples. The flow cytometer was calibrated before each experiment with QC beads (CytoFLEX Daily QC Fluorospheres, Beckman Coulter) to ensure comparable fluorescence values across experiments from different days. All flow cytometry data containing the more weakly expressing I_1–I_2 half sites contain more than 15,000 events in the used gate per individual sample. All flow cytometry data containing the more strongly expressing I_1–I_1 half sites had more than 15,000 events in the used gate per individual sample until an IPTG concentration of 15.625 µM. This covers all data from which we drew conclusions. The count number for samples with IPTG concentrations higher than 15.625 µM using the I_1–I_1 half sites deceased due to the slower growth caused by the toxicity of high gene expression, but in all cases we counted more than 500 counts in the used gate per individual sample. We used a 2D forward and side scatter gate, which was drawn by eye and corresponded to the experimentally determined size of the testing strain at logarithmic growth and was kept constant for the analysis of all experiments and used for calculations of the median and CV using CytExpert software. The same gating strategy has been used previously and is depicted in Extended Data Fig. 10.

Characterization of the FP1–FP8 VVD–AraC(DBD) fusion constructs. Overnight cultures of cells transformed with the FP1–FP8 fusions as well as the controls were diluted to OD_{600} = 0.1, allowed to grow in the dark to OD_{600} = 0.4 and split into two cultures, one of which was kept in the dark and one of which was illuminated for 4 h. The overnight culture of the negative control was diluted to OD_{600} = 0.1 and allowed to grow for the same amount of time as all other cultures (~5 h 30 min). The overnight cultures of the positive controls were diluted to OD_{600} = 0.1, allowed to grow to OD_{600} = 0.4 and split into two cultures, one of which was left without arabinose and one of which was induced with 0.1% arabinose for 4 h. After the induction time, 200 µl of each sample was collected, mixed with 200 µl of a transcription and translation inhibition solution (500 µg ml^{-1} rifampicin and 50 µg ml^{-1} doxycycline in PBS) and incubated in the dark for 90 min at 37 °C with 110 r.p.m. shaking. This protocol allowed use to obtain a full maturation of almost all the mCherry proteins translated at the end of the induction time[1]. After incubation with the inhibitor, samples were diluted 1:1 with 60% glycerol and frozen at −80 °C.

Dynamic control of gene expression. The overnight cultures transformed with pBLADE(FP6**)–mCherry, pReporter_only (negative control) and pBAD33–mCherry were diluted in TB to OD_{600} = 0.05 in dark tubes and glass transparent tubes, respectively, and allowed to grow until OD_{600} = 0.15, then 200 µl of each sample was collected, mixed with 200 µl of a transcription and translation inhibition solution (500 µg ml^{-1} rifampicin and 50 µg ml^{-1} doxycycline in PBS), incubated in the dark for 90 min at 37 °C with 110 r.p.m. shaking, diluted 1:1 with 60% glycerol, and frozen at −80 °C. The rest of the culture was transferred into transparent glass tubes. The culture with BLADE was illuminated with blue light (as described in the 'Light illumination systems' section) for 2 h, while the culture with pBAD33 was split into three different tubes and induced with different arabinose concentrations for 2 h. Then, aliquots from all the samples were taken and frozen with 60% glycerol 1:1. The remaining culture transformed with pBLADE(FP6*)–mCherry was diluted to OD_{600} = 0.15 with pre-warmed TB and transferred to a dark tube, while the cultures transformed with pBAD33–mCherry were centrifuged at 6,000*g* for 4 min and resuspended with the same volume of TB. The centrifugation and resuspension steps were repeated a second time to further remove the arabinose from the medium, and the cultures were transferred to another glass tube. All cultures were subjected to a total of three cycles.

Measurement of the kinetics of BLADE- and AraC-mediated mCherry expression. Chemically competent *E. coli* MG1655 cells were transformed with pBLADE(FP6*)–mCherry, pReporter_only and pBAD33–mCherry. The overnight cultures were diluted to OD_{600} = 0.1 and allowed to grow in the dark to OD_{600} = 0.4, then 100 µl of each sample was collected, mixed with 100 µl of a transcription and translation inhibition solution (500 µg ml^{-1} rifampicin and 50 µg ml^{-1} doxycycline in PBS), incubated in the dark for 90 min at 37 °C with 110 r.p.m. shaking, diluted 1:1 with 60% glycerol, and frozen at −80 °C. The culture transformed with pBLADE was then split into four tubes, of which three were induced with blue light of different intensities and one was kept in the dark. The cultures transformed with pBAD33–mCherry were split into four cultures, of which three were induced with different arabinose concentrations and one was kept without arabinose. Every hour for 6 h, 100 µl of each sample was collected, mixed with 100 µl of the transcription and translation inhibition solution, incubated in the dark for 90 min at 37 °C with 110 r.p.m. shaking, diluted 1:1 with 60% glycerol, frozen at −80 °C and subsequently analyzed with the flow cytometer.

Light intensity titration. Chemically competent *E. coli* MG1655 cells were transformed with pBLADE(FP6**)–mCherry and pReporter_only. The overnight culture of the cells transformed with pBLADE(FP6**)–mCherry was diluted and split into five independent cultures, each of which was induced with blue light of different intensity (tuned by adjusting the voltage in the power supply connected to the LEDs) for 4 h. The overnight culture of the cells transformed with pReporter_only was diluted and grown in the dark for 4 h, then 200 µl of each sample was collected, mixed with 200 µl of the transcription and translation inhibition solution, incubated in the dark for 90 min at 37 °C with 110 r.p.m. shaking, diluted 1:1 with 60% glycerol, frozen at −80 °C and subsequently analyzed with the flow cytometer.

Bacterial photography. Chemically competent *E. coli* MG1655 cells were transformed with pBLADE(FP6*)–sfGFP. The overnight culture was diluted in LB medium to OD_{600} = 0.1 and grown for ~6 h. A 96-well lid (12.7 × 8.5 cm) was filled with 30–40 ml of 1% LB–agar and allowed to solidify, then 1 ml of the culture was mixed with 9 ml of 0.4% agar at 42 °C (measured with a TFA Dostmann infrared thermometer, Wertheim) and plated on top of the solidified agar in the 96-well lid. The plate was covered with a transparent Plexiglass sheet (12.5 × 8.3 cm) with the Blade Runner movie poster sticker. For the bacteriograph of Michelangelo's 'Creation of Adam', the same protocol was followed, but 350–400 ml of 1% LB–agar were poured in an 18 × 15-cm case, for a total photomask area of 15.5 × 9 cm. The plates were then placed in a 37 °C incubator under blue light overnight. The next morning, the plates were imaged with a Zeiss Axio Zoom.V16 stereo zoom microscope equipped with a Plan-NeoFluar Z ×1.0 objective, zoom ×0.7, AxioCam MR R3 camera and a 38 HE filter set (ex. BP 470/40, FT 495, em. BP 525/50; sfGFP).

DIC and fluorescence microscopy. A 5-µl volume of the bacterial culture was applied to a thin agarose pad composed of 1% agarose for microscopy at room temperature and of 1% agarose and 0.1% LB medium in tethering buffer (10 mM potassium phosphate, 0.1 mM EDTA, 1 mM L-methionine and 10 mM sodium lactate; pH 7.0) for long-term microscopy at 37 °C. Images were acquired on a Zeiss Axio Observer Z1/7 fluorescence microscope equipped with a Colibri 7 LED light source, an Alpha Plan-Apochromat ×100/1.46 oil DIC (UV) M27 objective, filter sets 38 HE (ex. Band Pass [BP] 470/40, dichroic beamsplitter [farbteiler, FT] 495, em. BP 525/50; sfGFP), Filter set 108 High Efficiency (HE) (ex. BP 423/44, Dual Beam Splitter[DBS] 450 + 538, em. Double Band Pass [DBP] 467/24 + 598/110; MM 4–64), 96 HE (ex. BP 390/40, FT 420, em. BP 450/40; DAPI) and 64 HE (ex. BP 587/25, FT 605, em. BP 647/70; mCherry) and an Axiocam 506 Mono camera.

The induction of gene expression in selected cells within a population of MG1655 cells transformed with pBLADE(FP6**)–sfGFP was performed on a Zeiss LSM 800 confocal microscope. An area of 6.4 µm^2 was illuminated with a 488-nm diode laser (10 mW) at 0.1% intensity, with a frame average of 8, resulting in 0.36 µs of light per pixel. The illumination was given in pulses of 5 min for a duration of 3 h.

Fluorescence recovery after photobleaching. The overnight culture was diluted in the morning in fresh TB to OD_{600} = 0.1, and grown until it reached OD_{600} = 0.4, then 5 µl of the culture were applied to a thin 1% agarose pad. Cells showing foci were manually selected. The whole fluorescent focus was bleached with a single 1-s pulse of a 488-nm diode laser (10 mW) at 50% intensity on a Zeiss LSM 800 confocal microscope. Images in the GFP channel (filter set 38 HE: ex. BP 470/40, FT 495, em. BP 525/50) were taken before, immediately and 15-min post bleaching.

Induction of *rodZ* in KC717 cells. Strain KC717 (kind gift of K.C. Huang, Stanford University) was grown in LB medium supplemented with 0.2% arabinose (to keep the cells rod-shaped) during the preparation of chemically competent cells and culturing for DNA extraction procedures. The blue light and arabinose induction were performed as described above. The recovery phase of the culture induced with arabinose was performed by centrifuging the cells at 4,000*g* for 4 min and resuspending them with the same volume of LB medium twice. The culture was then diluted to OD_{600} = 0.1. The recovery phase of the culture transformed with pBLADE^{ONLY_C} (based on pBAD33) was performed by dilution to OD_{600} = 0.1 and incubation in the dark.

BLADE (FP6) expression and purification. Chemically competent *E. coli* Rosetta (DE3) cells carrying the pLysS plasmid were freshly transformed with pET28a–FP6 and cultivated overnight in LB medium supplemented with 50 µg ml^{-1} kanamycin. A daily culture was grown in LB medium with kanamycin at 37 °C until OD_{600} = 0.5, after which 1 mM IPTG and 5 µM FAD were added, and the culture was grown for 16 h at 18 °C under constant blue light. Cells were collected by centrifugation and the pellet was resuspended in 30 ml of lysis buffer (50 mM potassium phosphate pH 8.0, 300 mM NaCl and 10 mM imidazole pH 8.0) supplemented with a cOmplete protease inhibitor cocktail tablet (Roche). Cell lysis was performed by sonication and the lysate was centrifuged at 20,000 r.p.m. for 20 min at 4 °C. The supernatant was then incubated with 1 ml of HisPur Ni-NTA resin (Thermo Scientific) for 2 h at 4 °C. Protein purification was performed by the gravity flow method. The bound proteins were washed twice with 5 ml of wash buffer (lysis buffer + 10% glycerol + 20 mM imidazole) and finally eluted with 1.5 ml of elution buffer (50 mM potassium phosphate pH 7.5, 300 mM NaCl, 500 mM imidazole pH 8.0 and 10% glycerol). The elution buffer was replaced with a storage buffer (20 mM HEPES-NaOH pH 7.5, 150 mM NaCl and 10% glycerol) using an Amicon Ultra-4 regenerated cellulose (nominal molecular weight limit 10 kDa) centrifugal filter unit (Merck). The protein was then stored as 50-µl aliquots at −80 °C.

Spectroscopy. The absorption spectrum of the FAD cofactor bound to VVD within BLADE (FP6) was measured by exciting the sample in the 300–600-nm range using a Multiskan GO (Thermo Scientific) plate reader. The protein sample was incubated for four days at 4 °C in the dark in a buffer solution (25 mM HEPES, 150 mM NaCl, 10% glycerol, 0.1% EDTA; pH 7.5) and then diluted to 0.5 mg ml^{-1}. The same sample was then illuminated with blue light (455 nm, 50 W m^{-2}) for 5 min at room temperature and the absorption spectrum in the lit state was measured. The absorption spectrum of the blank (only medium) was subtracted from the dark and lit state spectra.

Size-exclusion chromatography. Purified BLADE (FP6) was thawed and stored in complete darkness at 4 °C for six days. The sample (1 ml of protein with a concentration of 0.5 mg ml^{-1}) was loaded onto a Superdex 75 Increase 10/300 GL (GE Healthcare Lifesciences) column at 4 °C. The running buffer consisted of 20 mM HEPES-NaOH pH 7.5, 150 mM NaCl and 10% glycerol, and the flow rate was adjusted to 0.25 ml min^{-1}. For the lit sample, the protein was incubated under constant blue light (455 nm, 50 W m^{-2}) for 30 min at 4 °C, before injection. During the run, the column was either illuminated with constant blue light (460 nm, 8 W m^{-2}, lit sample) or kept in complete darkness (dark sample). BSA and carbonic anhydrase were used as molecular markers at a concentration of 0.5 mg ml^{-1} each.

Quantification of cell length, width and roundness. The cell length and width were calculated by first staining the cell with the membrane dye MM 4–64 (AAT Bioquest) to visualize the cell contour, and then manually measuring the long and short axes of the cell, respectively, using the straight-line 'Selection' tool of Fiji (v. 2.0.0). The histograms were generated in Excel (2019) with the Analysis ToolPak's Histogram option. The roundness was calculated in Fiji using the formula $4\times(\text{area})/(\pi\times(\text{major axis})^2)$ after manually setting the oval 'Selection' tool on each cell.

Mathematical modeling. The LacI IPTG dose response was fitted to a Hill equation of the following form:

$$f(x) = r_{\max}\frac{x^n}{k_m + x^n}$$

where $f(x)$ describes the gene expression controlled by LacI, x represents the IPTG concentration, r_{max} is the maximal promoter expression, k_m is IPTG's dissociation constant for LacI and n is the Hill coefficient for LacI. This dose response was used subsequently to obtain IPTG concentration estimates from the fluorescence readouts of the constitutive promoters. All data were fitted using a nonlinear least-squares optimizer (MATLAB v. R2015a 8.5.0.197613, MathWorks) with fitted parameter values $r_{max} = 21{,}352$, $k_m = 62$ and $n = 1.7$.

Growth on L-arabinose. Cultures were inoculated from glycerol stocks and grown for 24 h in M9 medium supplemented with 0.001% thiamine, 0.00006% ferric citrate, 0.1 mM calcium chloride, 1 mM magnesium sulfate. 2× M9 medium supplemented with 0.001% casamino acids, 0.002% thiamine, 0.00012% ferric citrate, 0.2 mM calcium chloride and 2 mM magnesium sulfate was prepared. Either 2 ml of 20% L-arabinose in H_2O or 2 ml of H_2O was added to 8 ml of medium to create medium containing 4% L-arabinose or no L-arabinose medium. IPTG was serially diluted starting with 4 mM IPTG using the 2× M9 medium. A 100 µl volume of preculture ($OD_{600} \approx 0.2$) was used for inoculation of 10 ml of main culture containing un-supplemented M9 medium. A 100 µl volume of inoculated medium was mixed with 100 µl 2× M9 medium and the respective concentration of IPTG and L-arabinose directly into the microplates. Culture (200 µl per well) was incubated in clear-bottomed 96-well plates (Cell Culture Microplates 96 Well µClear CELLSTAR, Greiner Bio-One, cat. no. 655090), which were sealed with peelable foil (sealing foil, clear peelable for PlateLoc, no. 16985-001, Agilent) to prevent liquid evaporation and guarantee sterility, as well as a plastic lid (Greiner Bio-One, cat. no. 656171). For pre- and main cultures, 34 µg ml^{-1} chloramphenicol was used. Cultures were grown at 37 °C with shaking at 300 r.p.m. as described in the 'Bacterial growth' section. The optical density of the samples was measured at 600 nm and with 9-nm bandwidth, using a Tecan Infinite 200Pro and Firmware v. 3.40 in absorbance mode, with 2×2 reads per well (square filled), 2,300-µm border, 10 flashes and settle time of 200 ms. The mean of the four measurement was used. All growth experiments, except for the light titration, were performed in triplicates and on two different days. For the light titration experiments, the same initial culture was aliquoted and incubated under the respective light conditions.

Reporting Summary. Further information on research design is available in the Nature Research Reporting Summary linked to this Article.

Data availability

pBLADE(FP6*)–mCherry, pBLADE(FP6**)–mCherry, pBLADEONLY_A and pBLADEONLY_C have been deposited at Addgene (IDs 168048, 168049, 168050 and 168051, respectively). All other plasmids constructed in this study are also available from the corresponding authors upon reasonable request. Source data are provided with this paper.

References

48. Baba, T. et al. Construction of *Escherichia coli* K-12 in-frame, single-gene knockout mutants: the Keio collection. *Mol. Syst. Biol.* **2**, 2006.0008 (2006).
49. Datsenko, K. A. & Wanner, B. L. One-step inactivation of chromosomal genes in *Escherichia coli* K-12 using PCR products. *Proc. Natl Acad. Sci. USA* **97**, 6640–6645 (2000).
50. Bowers, L. M., Lapoint, K., Anthony, L., Pluciennik, A. & Filutowicz, M. Bacterial expression system with tightly regulated gene expression and plasmid copy number. *Gene* **340**, 11–18 (2004).
51. Guyer, M. S., Reed, R. R., Steitz, J. A. & Low, K. B. Identification of a sex-factor-affinity site in *E. coli* as gamma delta. *Cold Spring Harb. Symp. Quant. Biol.* **45**, 135–140 (1981).
52. Potapov, V. et al. Comprehensive profiling of four base overhang ligation fidelity by T4 DNA ligase and application to DNA assembly. *ACS Synth. Biol.* **7**, 2665–2674 (2018).
53. Chung, C. T., Niemela, S. L. & Miller, R. H. One-step preparation of competent *Escherichia coli*: transformation and storage of bacterial cells in the same solution. *Proc. Natl Acad. Sci. USA* **86**, 2172–2175 (1989).
54. Gerhardt, K. P. et al. An open-hardware platform for optogenetics and photobiology. *Sci. Rep.* **6**, 35363 (2016).
55. Szeto, T. H., Rowland, S. L., Habrukowich, C. L. & King, G. F. The MinD membrane targeting sequence is a transplantable lipid-binding helix. *J. Biol. Chem.* **278**, 40050–40056 (2003).
56. Doi, M. et al. Determinations of the DNA sequence of the *mreB* gene and of the gene products of the mre region that function in formation of the rod shape of *Escherichia coli* cells. *J. Bacteriol.* **170**, 4619–4624 (1988).
57. van den Ent, F., Johnson, C. M., Persons, L., de Boer, P. & Lowe, J. Bacterial actin MreB assembles in complex with cell shape protein RodZ. *EMBO J.* **29**, 1081–1090 (2010).
58. Kruse, T., Moller-Jensen, J., Lobner-Olesen, A. & Gerdes, K. Dysfunctional MreB inhibits chromosome segregation in *Escherichia coli*. *EMBO J.* **22**, 5283–5292 (2003).
59. Lou, C., Stanton, B., Chen, Y. J., Munsky, B. & Voigt, C. A. Ribozyme-based insulator parts buffer synthetic circuits from genetic context. *Nat. Biotechnol.* **30**, 1137–1142 (2012).

Acknowledgements

We thank M. Hörner for his help with determination of the absorption spectrum of BLADE, J. Nuno de Sousa Machado for his help with size-exclusion chromatography, Y. Weber for help with characterizing the 96-well light induction plate, K.C. Huang for sharing with us the KC717 strain and S. Aoki for helpful discussions. This study was funded by the DFG (grant no. VE776/2-1 to B.D.V.), by the BMBF (grant no. 031L0079 to B.D.V.), by the Excellence Initiative of the German Federal and State Governments BIOSS (Centre for Biological Signalling Studies; EXC-294), by the European Research Council (ERC-Advanced) under the European Union's Horizon 2020 research and innovation program (grant agreement no. 743269) and a FET-Open research and innovation actions grant under the European Union's Horizon 2020 research and innovation program (CyGenTiG; grant agreement no. 801041).

Author contributions

B.D.V. and A.B. conceived the study. B.D.V. and M.K. supervised the study, and secured funding. E.R., A.B., E.B.A., N.P., M.K. and B.D.V. designed experiments and interpreted the data. E.R., A.B., M.H. and E.B.A. performed in vivo experiments. N.P. purified BLADE, and performed size-exclusion chromatography. L.E. performed the initial experiments, which validated the idea. G.S. developed the 96-well light set-up in collaboration with A.B. M.A.Ö. performed bioinformatics and computational structural biology analyses of the BLADE constructs. E.R., A.B., M.K. and B.D.V. wrote the manuscript.

Competing interests

The authors declare no competing interests.

Additional information

Extended data is available for this paper at https://doi.org/10.1038/s41589-021-00787-6.

Supplementary information The online version contains supplementary material available at https://doi.org/10.1038/s41589-021-00787-6.

Correspondence and requests for materials should be addressed to M.K. or B.D.V.

Reprints and permissions information is available at www.nature.com/reprints.

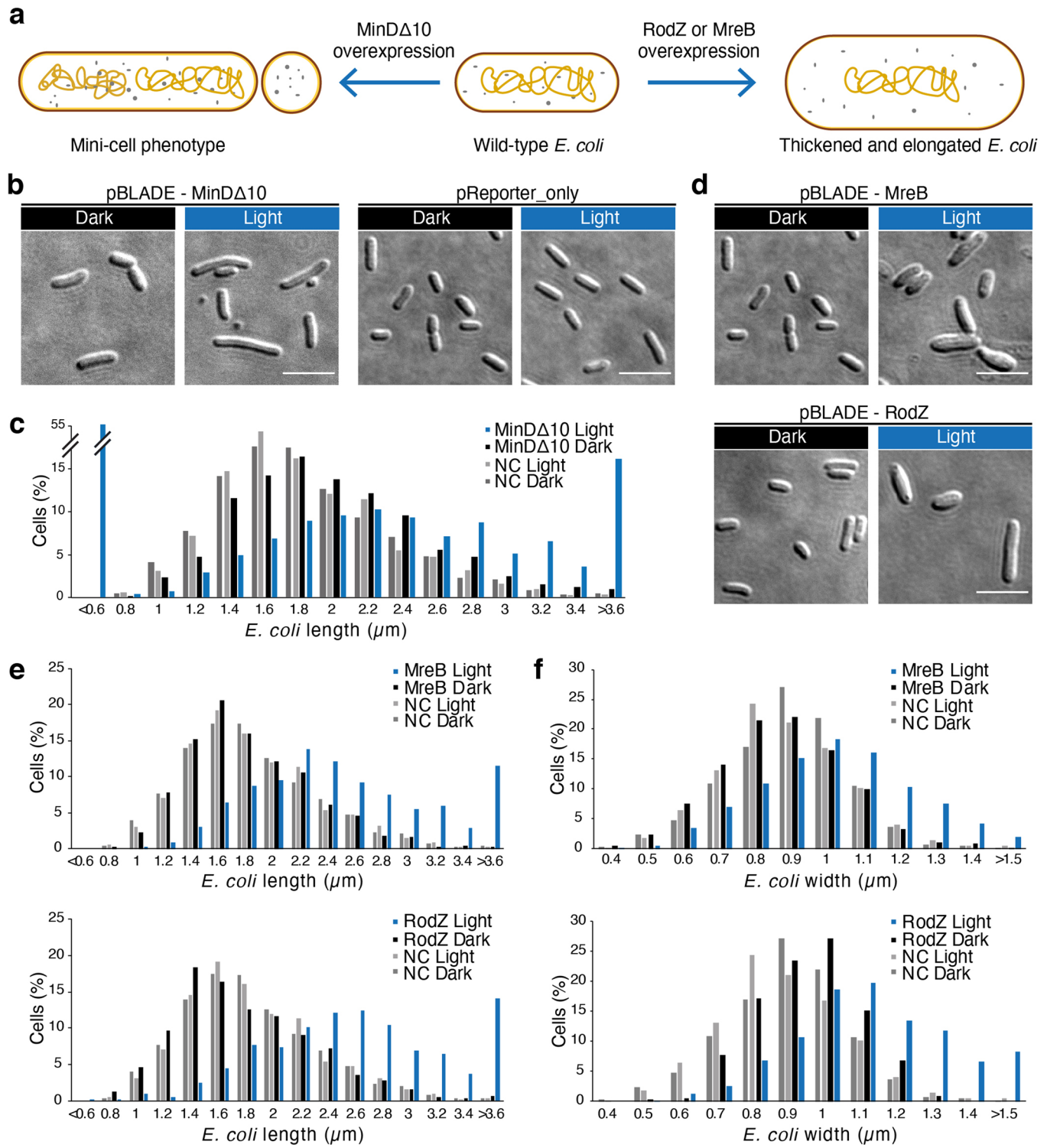

Extended Data Fig. 1 | See next page for caption.

Extended Data Fig. 1 | BLADE enables control of cell morphology. a, Expected phenotypes due to overexpression of the indicated proteins. MinDΔ10 is a truncated form of the cell division MinD lacking the C-terminal membrane targeting sequence (MTS). Without the MTS, MinDΔ10 cannot associate with the membrane and remains cytoplasmic. It however maintains the ability to homodimerize[26]. The heterodimer formed by MinD and MinDΔ10 is not able to stably bind to the membrane, because a monovalent MTS is not sufficient for this[55]. With MinD sequestered into the cytoplasm, endogenous MinC is no longer recruited to the membrane, and cannot counteract FtsZ, leading to the minicell phenotype. MreB is the bacterial actin homolog necessary for the establishment and maintenance of rod shape and cell wall synthesis[27,56]. Its assembly is regulated by RodZ, a transmembrane protein that binds MreB, altering the conformational dynamics and intrinsic curvature of MreB polymers[28,32,57]. It has been previously established that overexpression of MreB or RodZ leads to cell elongation and thickening[27,32,58]. **b**,**d**, Representative DIC images of *E. coli* MG1655 cells transformed with the indicated constructs grown for 4h either in the dark or under 460 nm light (5 W/m^2) illumination. Images were acquired on three days with the same results. Scale bar, 5 μm. **c**,**e**,**f**, Quantification of cell length and width distribution for the indicated samples and conditions. Values represent mean ± SD of $n = 3$ independent experiments. Note that the values for the negative control (NC; pReporter_only, see Supplementary Table 1) shown in (**c**) are shown again in (**e**) to allow for the easy comparison of the length distribution of all samples. Also in (**f**), the NC values are the same in the upper and lower graphs. The total number of analyzed cells is: NC Dark, 1022 cells (**c,e**), 782 (**f**); NC Light, 960 cells (**c,e**), 674 (**f**); MinDΔ10 Dark and Light, 880 cells; MreB Dark, 1016 cells (**e**, upper panel), 885 cells (**f**, upper panel); MreB Light, 962 cells (**e**, upper panel), 1006 cells (**f**, upper panel); RodZ Dark, 922 cells (**e**, lower panel), 885 cells (**f**, lower panel); RodZ Light, 941 cells (**e**, lower panel), 885 cells (**f**, lower panel). **b**-**f**, BLADE construct: FP4 driven by the J23101** promoter.

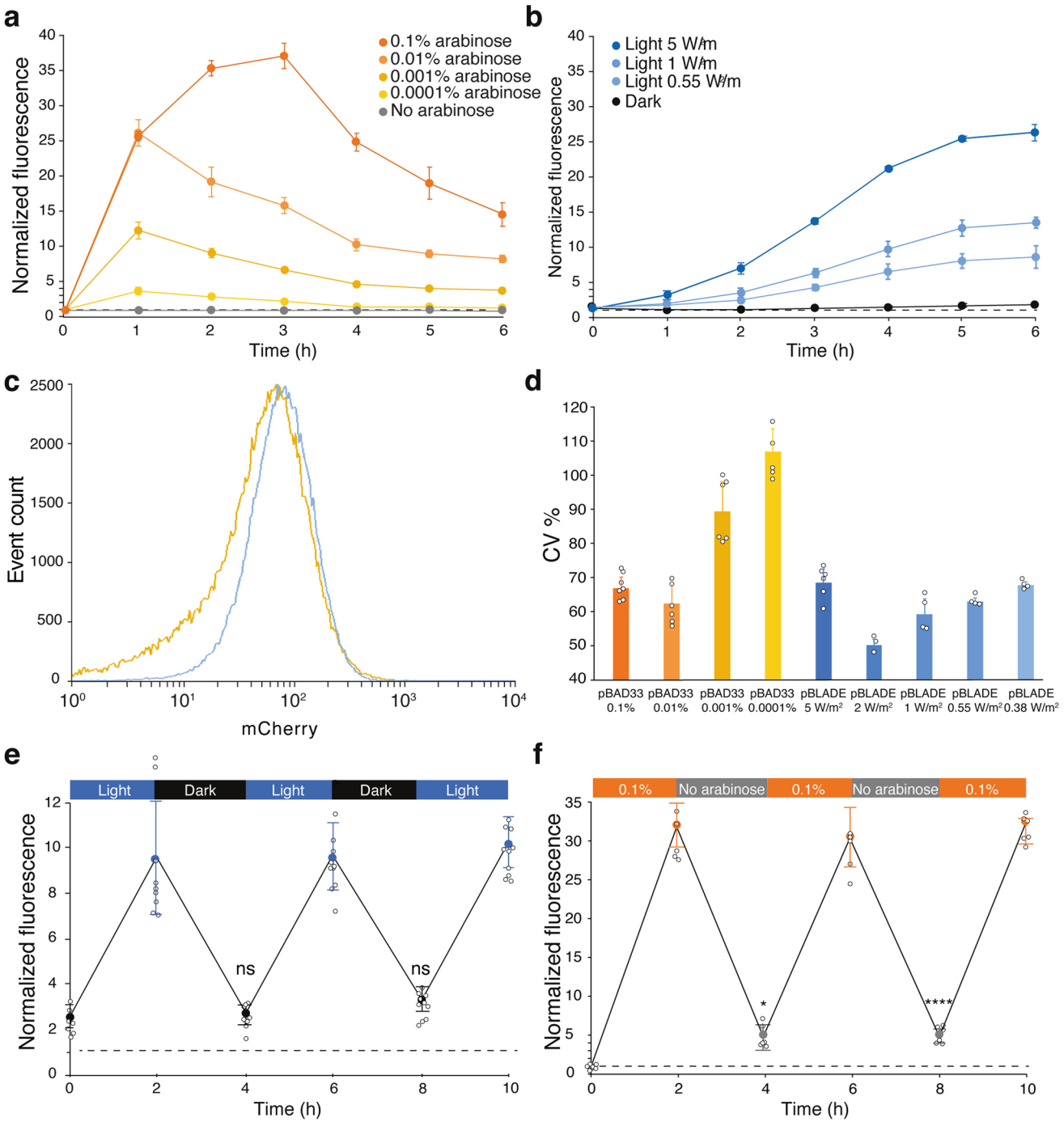

Extended Data Fig. 2 | Comparison between AraC and BLADE. a,**b**, Kinetics of mCherry expression in MG1655 cells transformed with pBAD33 (**a**) or pBLADE (**b**) and induced at t = 0 with the indicated arabinose concentrations or no arabinose (**a**) or with 460 nm light of the indicated intensities or left in the dark (**b**). **c**, Representative histograms showing the distribution of the mCherry fluorescence within a population of MG1655 cells transformed with either pBAD33 (orange) or pBLADE (pale blue) and induced for 4h with either 0.001% arabinose or with 0.38 W/m^2 of 460 nm blue light. **d**, Coefficient of variation (CV) of the mCherry fluorescence levels measured by flow cytometry in MG1655 cells transformed with either pBAD33 (shades of orange) or pBLADE (shades of blue) and induced 4h with the indicated concentrations of arabinose and light intensities, respectively. **e**, mCherry fluorescence intensity in MG1655 cells transformed with pBLADE after repeated cycles of blue light exposure (5 W/m^2) and darkness. **f-h**, mCherry fluorescence intensity in MG1655 cells transformed with pBAD33 after repeated cycles with the indicated arabinose concentration and without arabinose. **a-b**,**e-f**, All values were normalized to the mCherry fluorescence intensity measured in cells transformed with pReporter_only (see Supplementary Table 1; dashed line). **e**,**f**, From left to right, $P = 0.46738$ (**e**), $P = 0.05474$ (**e**), $P = 0.00007$ (**f**) and $P = 4.37 \times 10^{-9}$ (**f**). Not significant (ns), $P > 0.05$; single asterisk (*), $P < 0.05$; quadruple asterisk (****), $P < 0.0001$. P-values P were calculated by the two-tailed, homoscedastic Student's t test. Individual data points are the mean values of 10,000 single-cell flow cytometry events. **a,b,d-f**, Values represent mean ± SD of more than three biological replicates. BLADE constructs: FP6 fusion driven by the J23101* (**b-d**) or J23101** (**e**) promoter.

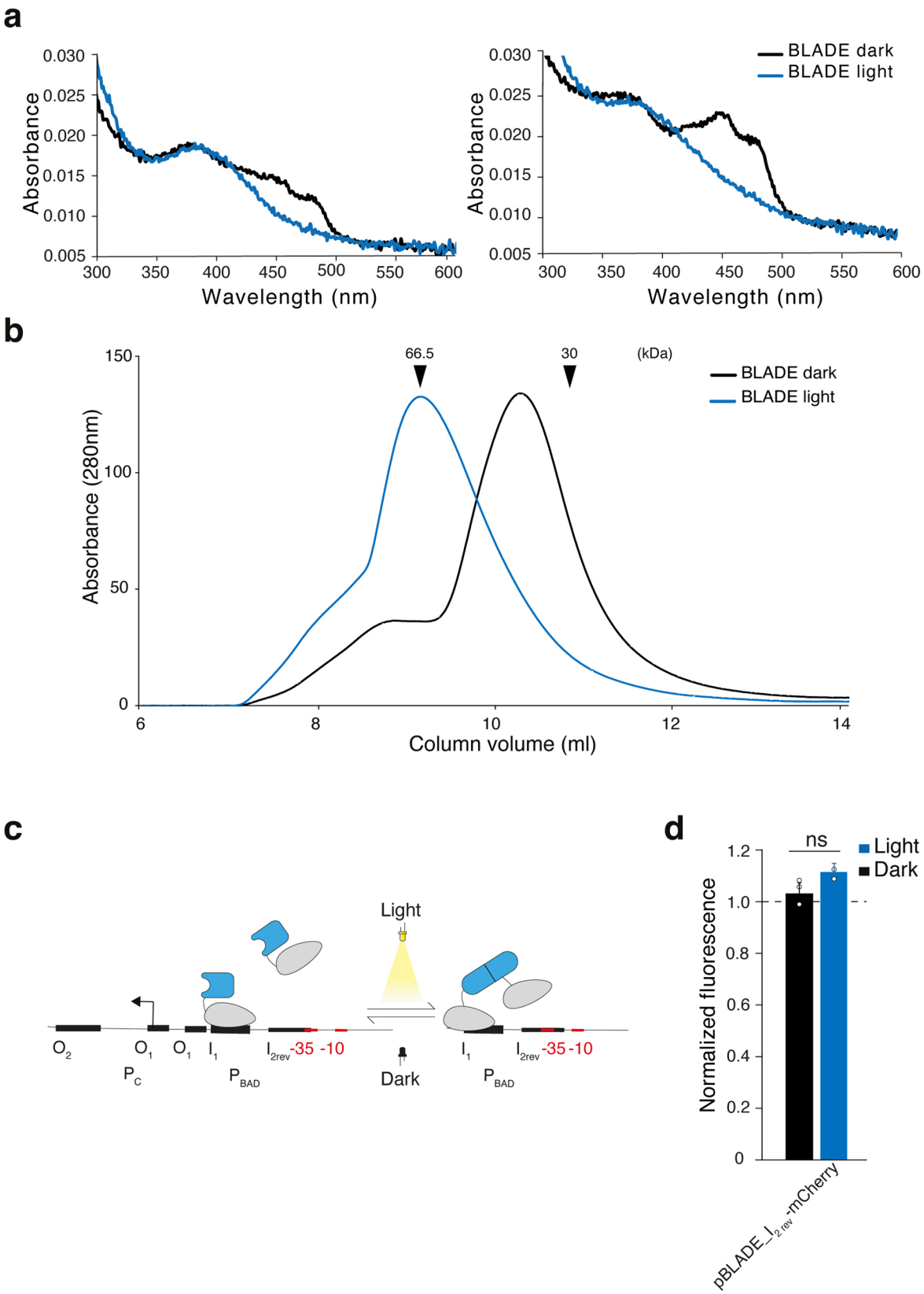

Extended Data Fig. 3 | See next page for caption.

Extended Data Fig. 3 | BLADE is dimeric under light and contacts the I2 DNA half-site. a, Absorption spectra measured with the protein incubated 1 day (left) or 4 days (right) in the dark at 4 °C (black) or illuminated with blue light (455 nm; 50 W/m^2) for 5 min at room temperature (cyan). The absorption spectrum of the blank (only medium) was subtracted from the dark and lit state spectra. **b**, SEC performed with purified BLADE in the dark or illuminated with 460 nm light (5 W/m^2) for 30 min at 4 °C. **c**, Schematic representation of the synthetic promoter with the inverted I_2 half-site. **d**, MG1655 cells transformed with pBLADE_$I_{2\ rev}$-mCherry grown 4h either in the dark or under 460 nm light (5 W/m^2) illumination were analyzed by flow cytometry. The values were normalized to the mCherry fluorescence intensity measured in cells transformed with pReporter_only (see Supplementary Table 1; dashed line). Values represent mean ± SD of $n = 3$ independent experiments. The individual data points are the mean values of 10,000 single-cell flow cytometry events. Not significant (ns), $P < 0.05$. The P-value P was calculated by the two-tailed, homoscedastic Student's t-test.

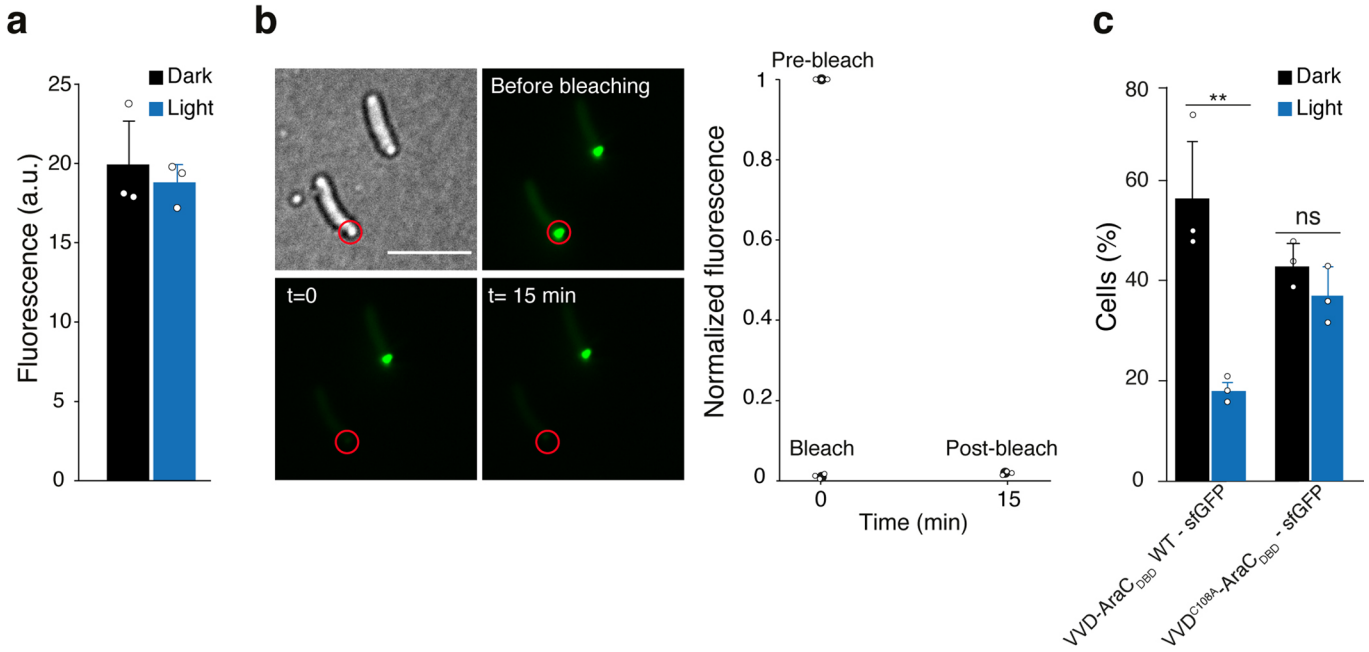

Extended Data Fig. 4 | The foci formed by BLADE-sfGFP in the dark are aggregates and are due to the VVD moiety. a, GFP fluorescence intensity measured in *E. coli* MG1655 cells transformed with a modified pBLADE in which BLADE was C-terminally fused with sfGFP grown for 4h in the dark or under 460 nm light (5 W/m^2) light. The individual data points are the mean values of 10,000 single-cell flow cytometry events. **b**, Left, representative images of a fluorescence recovery after photobleaching (FRAP) experiment. Scale bar, 5 μm. Right, Quantification of the recovery in three independent FRAP experiments. **c**, Quantification of the number of cells showing aggregates for the indicated constructs and conditions. From left to right, $P = 0.00451$ and $P = 0.09117$. Not significant (ns), $P < 0.05$; double asterisk (**), $P < 0.01$. P-values P were calculated by the two-tailed, homoscedastic Student's t-test. Values represent mean ± SD of $n = 3$ independent experiments. Total number of cells analyzed: $n = 670$ (VVD-AraC$_{DBD}$WT-sfGFP), and $n = 473$ (VVD^{C108A}-AraC$_{DBD}$-sfGFP).

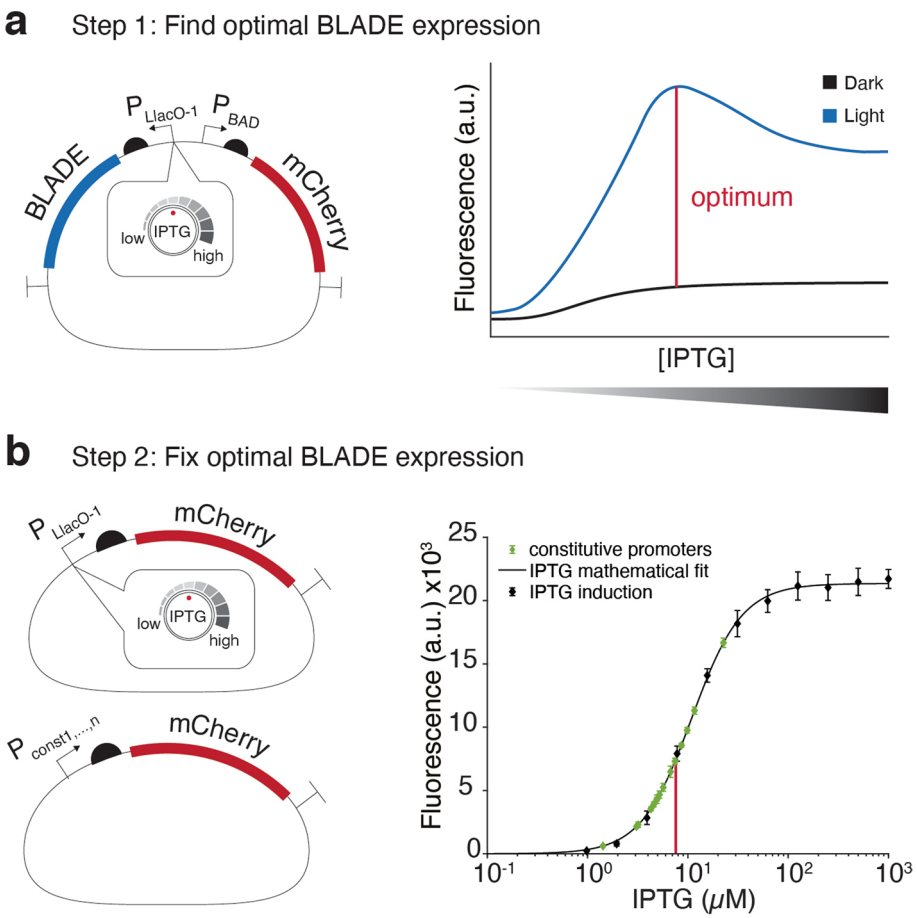

Extended Data Fig. 5 | Optimal gene expression output may be obtained at intermediate TF concentrations. a, Schematic representation of the plasmid used in step 1. Regulatory sequences (O_1 and O_2 half-sites) upstream of the P_{BAD} promoter have been deleted. Right, example of a scenario for which the highest mCherry levels are obtained at intermediate cTF levels (red line). **b**, In step 2, the range of transcriptional output (visualized through the fluorescent reporter expression) induced by different IPTG concentrations is mapped to the rates of constitutive promoters in a library (right), allowing for the identification of a constitutive promoter that matches the desired optimal BLADE expression level (schematically shown with a red line). A plasmid bearing the IPTG-inducible promoter as well as an extended library of constitutive promoters (http://parts.igem.org/Promoters/Catalog/Anderson) was used. To minimize the potential influence of individual promoters on mRNA transcription and translation initiation, we used a ribosome binding site (RBS) containing an insulating ribozyme (RiboJ[59]). Plotting the mCherry fluorescence levels obtained with the constitutive promoters and with the IPTG-inducible promoter at different IPTG concentrations in the same plot, it is possible to find the constitutive promoter that best matches the expression from the IPTG-inducible one at the desired IPTG concentration. This mapping has to be performed only once for a given strain background at specific conditions, which in our case as an example was done in *E. coli* BW25113*ΔaraC attB::lacY*. Values represent mean ± SD of more than three biological replicates acquired on different days.

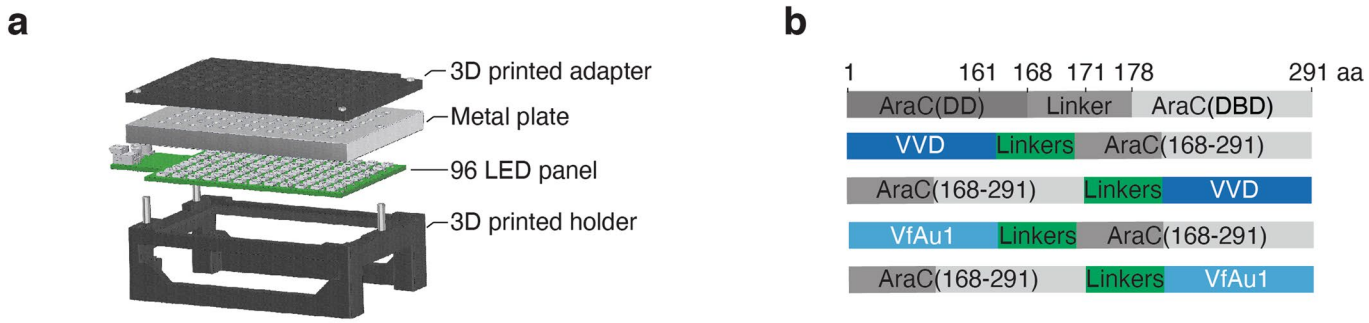

Extended Data Fig. 6 | Setup for the characterization of BLADE TFs. a, Light induction setup for 96-well microtiter plates containing a panel of 96 light emitting diodes (LEDs), 3D-printed holders and a metal plate for heat dissipation. The setup comprises a custom-made printed circuit board (PCB) with 96 individual LEDs of three different wavelengths (red, green and blue). Each LED can be controlled individually using a microcontroller, enabling the exposure of each well to the same light intensity, a crucial aspect for the characterization of the chimeric TFs. A milled metal plate placed in between the PCB and the LEDs dissipates the heat produced by the light induction device. A 3D-printed microplate adapter on top of the metal plate allows for the precise positioning of the 96-well plate. The light intensity of the device was calibrated using a Thorlabs PM100USB Power and Energy meter connected with a Thorlabs S170C Microscope Slide Power Sensor. **b**, Domain composition of the engineered light-inducible dimerization domain (VVD and VfAu1)-AraC(DBD) fusion constructs. 'Linkers' indicate a library of different synthetic linkers that were tested between the two domains.

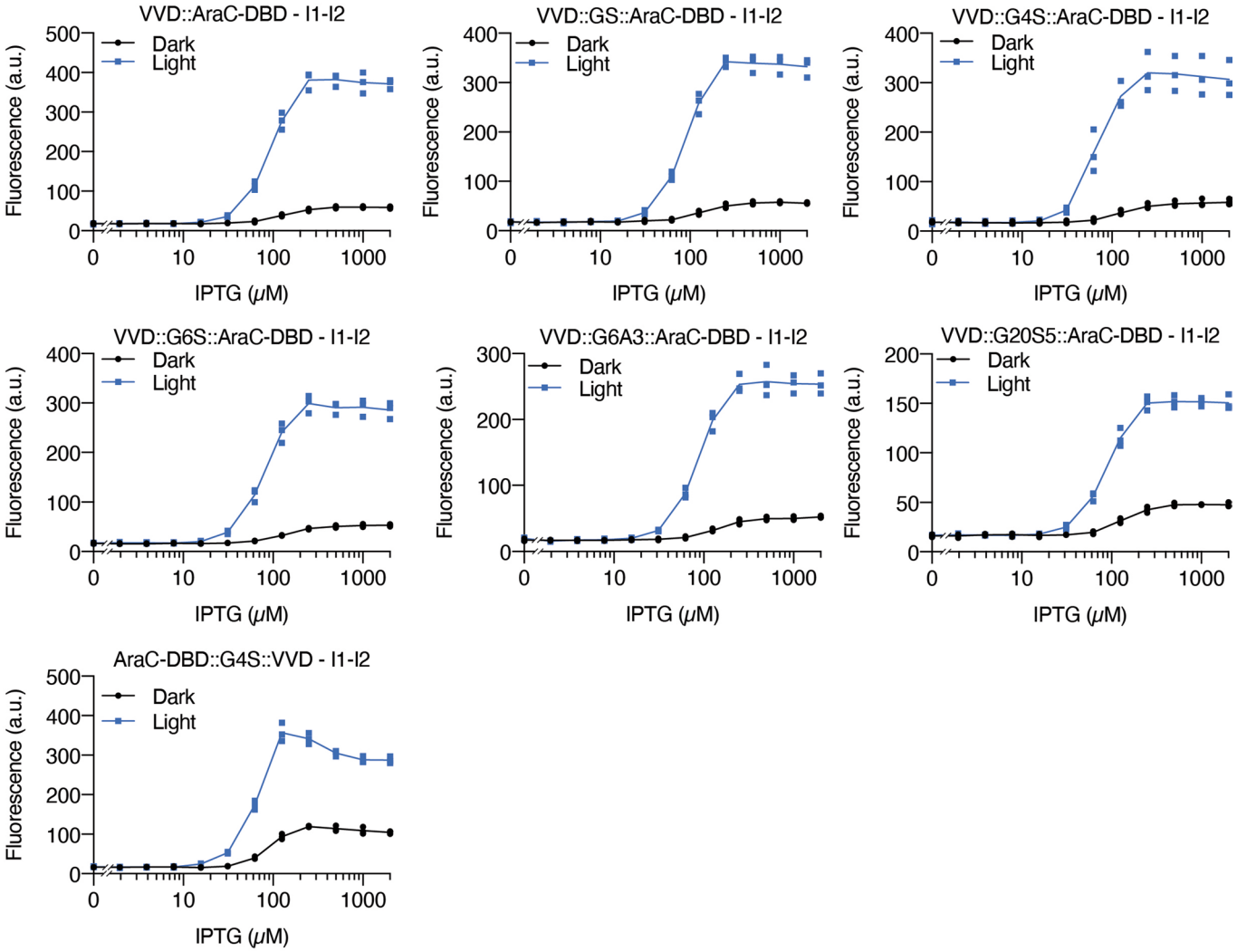

Extended Data Fig. 7 | IPTG-dose response curves for the VVD-AraC chimeric constructs. IPTG-dose response curves of cells transformed with the single plasmid bearing the indicated VVD-AraC fusions and mCherry under control of P_{BAD} deprived of all upstream regulatory elements. Cells were either kept in the dark, or illuminated with saturating blue light (465 nm; 3.85 W/m^2). The lines connect the mean mCherry fluorescence values of three individual samples, which are shown in blue squares for light induced samples and black dots for the dark control. For each condition, at least n = 3 individual experiments were performed, which are shown as individual points. Only the condition for fusion VVD::G4S::AraC(DBD) incubated at 1.953 μM IPTG and with light (465 nm; 3.85 W/m^2) contains two individual experiments (n = 2).

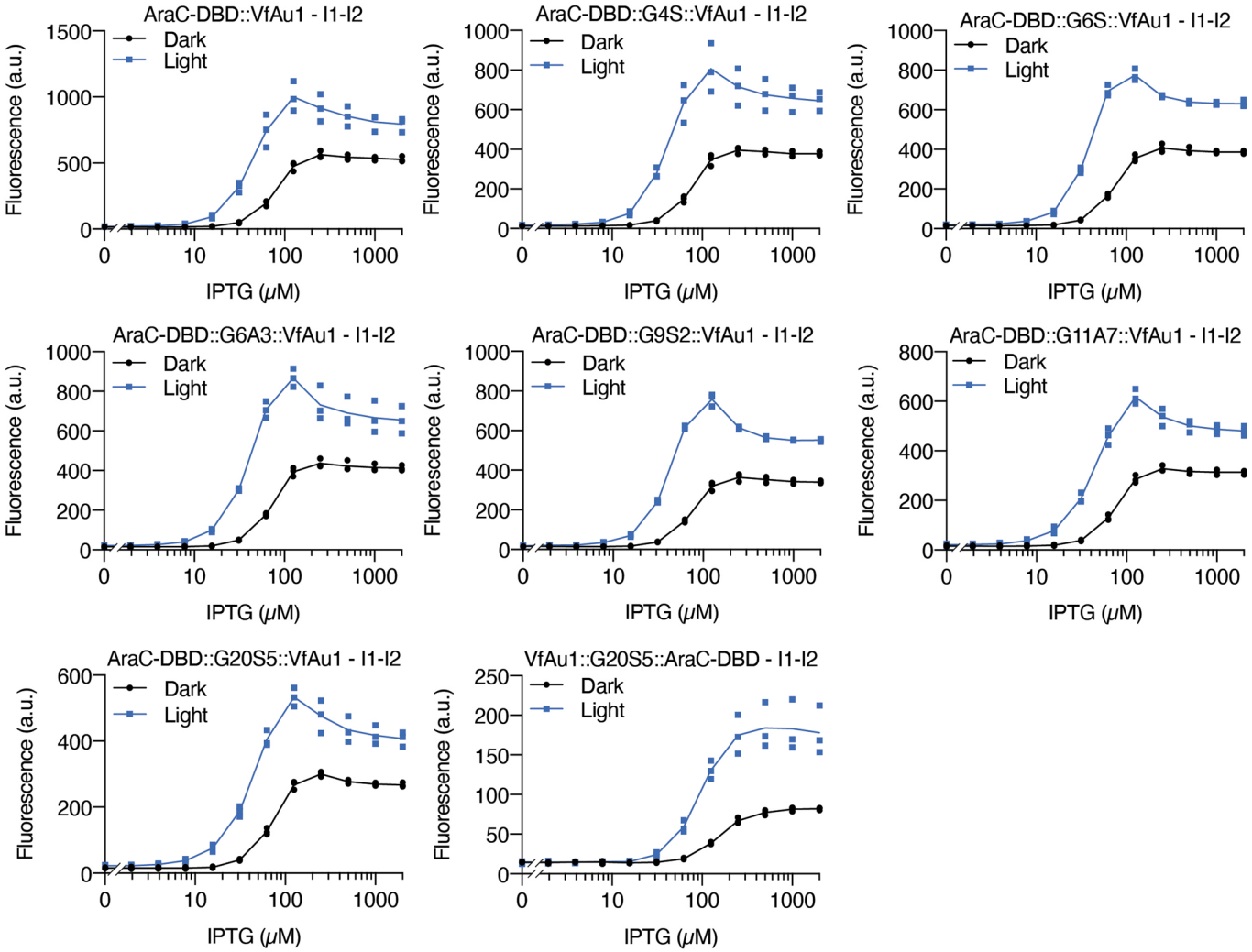

Extended Data Fig. 8 | IPTG-dose response curves for the VfAu1-AraC chimeric constructs. IPTG-dose response curves of cells transformed with the single plasmid bearing the indicated VfAu1-AraC fusions and mCherry under control of P_{BAD} deprived of all upstream regulatory elements. Cells were either kept in the dark, or illuminated with saturating blue light (465 nm; 3.85 W/m^2). The lines connect the mean mCherry fluorescence values of three individual samples, which are shown in blue squares for light induced samples and black dots for the dark control. For each condition, at least n = 3 individual experiments were performed, which are shown as individual points.

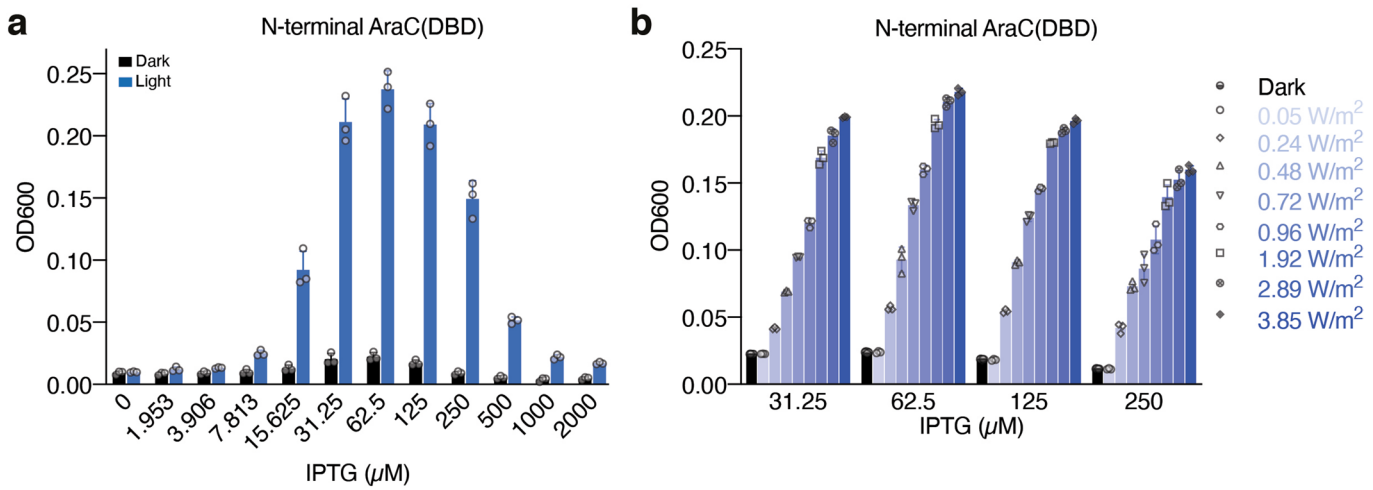

Extended Data Fig. 9 | IPTG- and light-dose response of AraC(DBD)::G_4S::VVD. a, Optical density of *E. coli* MG1655Δ*araC* cells expressing AraC(DBD)::G_4S::VVD grown for 18h at 37 °C in a medium containing 2% arabinose and the indicated IPTG concentrations either in the dark or under 465 nm light (3.85 W/m^2). **b**, Optical density of *E. coli* MG1655Δ*araC* cells expressing AraC(DBD)::G_4S::VVD grown for 17h20′ at 37 °C in a medium containing 2% arabinose and the indicated IPTG concentrations either in the dark or under 465 nm light of the indicated intensity. Bars represent mean ± SD of $n = 3$ biological replicates. Each data point shown in the bar plots represents a data point in a time course with measurements every 40 min, of which the average of the first three measurements was subtracted from all following time points to adjust for small differences in sample volume and inoculum. All time courses are shown in Supplementary Figs. 14 and 18.

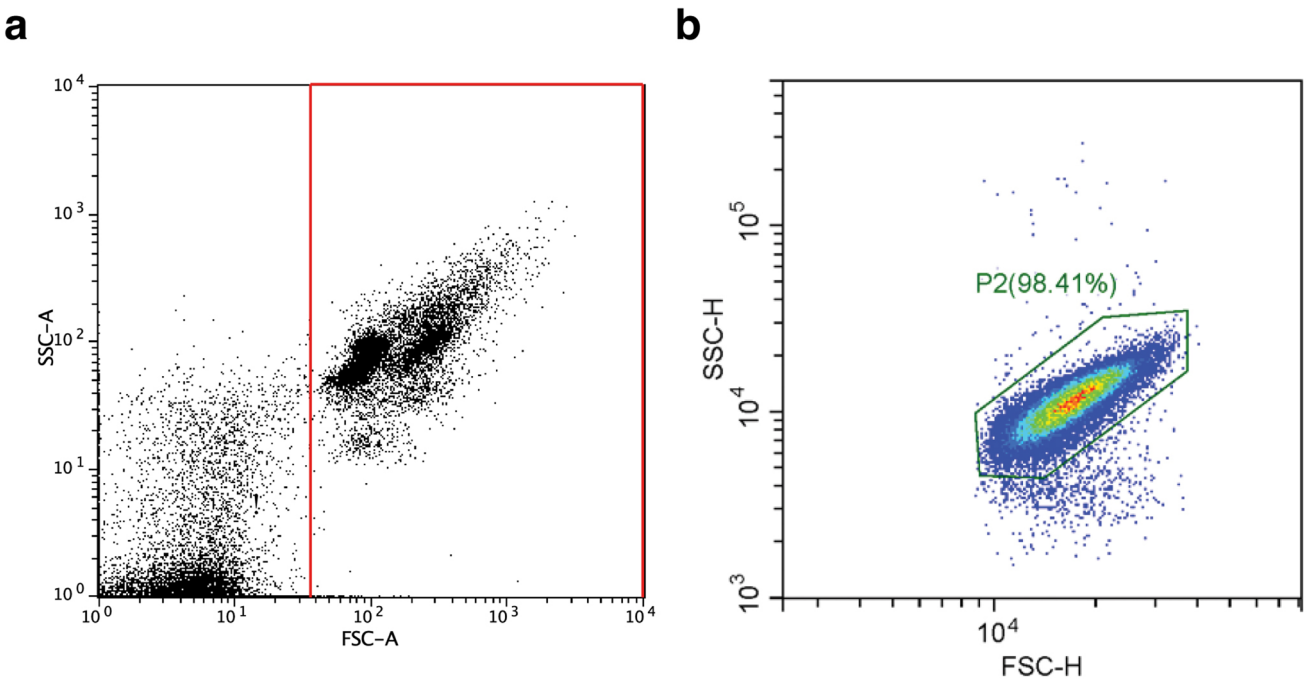

Extended Data Fig. 10 | Flow cytometry gating strategies. a, Screenshot of the gate used for the analysis of flow cytometric data shown in Figs. 1, 3, Extended Data Figs. 1–4 and Supplementary Figs. 3, 5 and 6 taken from the FCSalyzer v. 0.9.1.5 α software. The SSC-A and FSC-A rectangular gate used to eliminate the debris from the cell population was set on the control strain (MG1655 cells transformed with pReporter_only) on the BD Fortessa flow cytometer and was then kept constant for all other experiments using the same cell type. For each sample, 10,000 single cells residing in the selected area were analyzed. **b**, Screenshot of the gate used for the analysis of flow cytometric data shown in Fig. 5, Extended Data Figs. 7 and 8 and Supplementary Figs. 11 and 12 taken from the CytExpert software. The SSC-H and FSC-H hexagon gate was drawn by eye on a control strain (*E. coli* MG1655 *ΔaraCBAD ΔlacIZYA ΔaraE ΔaraFGH attB::lacYA177C ΔrhaSRT ΔrhaBADM Tn7::tetR kan(FRT)* in the CytExpert v.2.1.0.92 and then kept constant for all experiments using the same cell type.

nature research

Corresponding author(s): Mustafa Khammash and Barbara Di Ventura

Last updated by author(s): 05/03/2021

Reporting Summary

Nature Research wishes to improve the reproducibility of the work that we publish. This form provides structure for consistency and transparency in reporting. For further information on Nature Research policies, see our Editorial Policies and the Editorial Policy Checklist.

Statistics

For all statistical analyses, confirm that the following items are present in the figure legend, table legend, main text, or Methods section.

n/a	Confirmed	
☐	☒	The exact sample size (*n*) for each experimental group/condition, given as a discrete number and unit of measurement
☐	☒	A statement on whether measurements were taken from distinct samples or whether the same sample was measured repeatedly
☐	☒	The statistical test(s) used AND whether they are one- or two-sided *Only common tests should be described solely by name; describe more complex techniques in the Methods section.*
☒	☐	A description of all covariates tested
☒	☐	A description of any assumptions or corrections, such as tests of normality and adjustment for multiple comparisons
☐	☒	A full description of the statistical parameters including central tendency (e.g. means) or other basic estimates (e.g. regression coefficient) AND variation (e.g. standard deviation) or associated estimates of uncertainty (e.g. confidence intervals)
☐	☒	For null hypothesis testing, the test statistic (e.g. *F*, *t*, *r*) with confidence intervals, effect sizes, degrees of freedom and *P* value noted *Give P values as exact values whenever suitable.*
☒	☐	For Bayesian analysis, information on the choice of priors and Markov chain Monte Carlo settings
☒	☐	For hierarchical and complex designs, identification of the appropriate level for tests and full reporting of outcomes
☒	☐	Estimates of effect sizes (e.g. Cohen's *d*, Pearson's *r*), indicating how they were calculated

Our web collection on statistics for biologists contains articles on many of the points above.

Software and code

Policy information about availability of computer code

Data collection	FCSalyzer software (version: 0.9.1.5 alpha); CytExpert software (version: 2.1.092); Zen Blue software (version: 2.3); Tecan infinite 200Pro Firmware (version: 3.40)
Data analysis	Fiji (version: 2.0.0); Matlab (version: R2015a 8.5.0.197613); Excel (version:2019)

For manuscripts utilizing custom algorithms or software that are central to the research but not yet described in published literature, software must be made available to editors and reviewers. We strongly encourage code deposition in a community repository (e.g. GitHub). See the Nature Research guidelines for submitting code & software for further information.

Data

Policy information about availability of data

All manuscripts must include a data availability statement. This statement should provide the following information, where applicable:

- Accession codes, unique identifiers, or web links for publicly available datasets
- A list of figures that have associated raw data
- A description of any restrictions on data availability

Some of the plasmids constructed in this study have been deposited on Addgene (pBLADE(FP6*)-mCherry, pBLADE(FP6**)-mCherry, pBLADEONLY_A and pBLADEONLY_C). All other plasmids constructed in this study will be additionally available from the corresponding authors upon reasonable request. We created source data files to support all the conclusions of the paper.

Field-specific reporting

Please select the one below that is the best fit for your research. If you are not sure, read the appropriate sections before making your selection.

☒ Life sciences ☐ Behavioural & social sciences ☐ Ecological, evolutionary & environmental sciences

For a reference copy of the document with all sections, see nature.com/documents/nr-reporting-summary-flat.pdf

Life sciences study design

All studies must disclose on these points even when the disclosure is negative.

Sample size	the size of the experiment was estimated from preliminary test experiments
Data exclusions	in flow cytometry, debris was excluded from the analysis.
Replication	The experiments whose results are shown in Supplementary Figs. 4a, and, as indicated in the figure legends, one condition in Extended Data Fig.7 and Supplementary Fig. 12, were performed twice - both times with similar results. We performed all other experiments at least three times (three biological independent experiments, starting from different cultures). All the experiments led to similar results.
Randomization	no randomization was performed because we used genetically identical samples whenever comparisons were made
Blinding	blinding was not performed because the features we analyzed (fluorescence intensity, cell growth, chromatography results, etc.) are not subject to biased interpretation

Reporting for specific materials, systems and methods

We require information from authors about some types of materials, experimental systems and methods used in many studies. Here, indicate whether each material, system or method listed is relevant to your study. If you are not sure if a list item applies to your research, read the appropriate section before selecting a response.

Materials & experimental systems

n/a	Involved in the study
☒	☐ Antibodies
☒	☐ Eukaryotic cell lines
☒	☐ Palaeontology and archaeology
☒	☐ Animals and other organisms
☒	☐ Human research participants
☒	☐ Clinical data
☒	☐ Dual use research of concern

Methods

n/a	Involved in the study
☒	☐ ChIP-seq
☐	☒ Flow cytometry
☒	☐ MRI-based neuroimaging

Flow Cytometry

Plots

Confirm that:

☒ The axis labels state the marker and fluorochrome used (e.g. CD4-FITC).

☒ The axis scales are clearly visible. Include numbers along axes only for bottom left plot of group (a 'group' is an analysis of identical markers).

☒ All plots are contour plots with outliers or pseudocolor plots.

☒ A numerical value for number of cells or percentage (with statistics) is provided.

Methodology

Sample preparation	Samples were centrifuged at 4000g for 4 min to remove the glycerol-containing solution, then the pellets were resuspended in PBS.
Instrument	LSR Fortessa flow cytometer (BD Biosciences) and Cytoflex S flow cytometer (Beckman Coulter)
Software	FCSalyzer software and CytExpert 2.1.092 software
Cell population abundance	only a small fraction of debris was gated out of the analysis. the most abundant population was retained for analysis.

Gating strategy

With the LSR Fortessa a forward scatter height (FSC-H) threshold of 1,400 was used to gate for living cells and eliminate debris. With the Cytoflex S f thresholds of 2,500 FSC-H and 1,000 SSC-H were used for all samples.

☒ Tick this box to confirm that a figure exemplifying the gating strategy is provided in the Supplementary Information.